JOURNAL OF GEOPHYSICAL RESEARCH, VOL. ???, XXXX, DOI:10.1029/,

Hindcasting the Adriatic Sea near-surface motions with a coupled wave-current model

M. Dutour Sikirić[1], A. Roland[2], I. Tomažić[1], M. Kuzmić[1], and I. Janeković[1]

[1]Department of Marine and Environmental Research, Rudjer Bošković Institute, Bijenička 54, 10000 Zagreb, Croatia

[2]Institute of Hydraulic and Water Resources Engineering, Technische Universität Darmstadt, Darmstadt, Germany

Abstract. Prediction of near-surface motion is one of the most challenging problems in oceanography because of the combined effects of waves, currents and turbulence. In this work an implementation of the Regional Ocean Modelling System (ROMS), two-way coupled to the Wind Wave Model III (WWM-III), is used as the computational platform for the numerical experiments designed to elucidate the wave contribution to modeling the movements near the air-sea interface. To that end we apply the latest concepts in physics of spectral wave models to close the momentum balance in the surface boundary layer. To force the ROMS and WWM-II models and to assess their modeling skill we draw on parts of the huge database of observational and simulation data put together during 2002-2003 when scientists from several countries conducted intensive multi-disciplinary research of the Adriatic. When all contributions were accounted for, comparison of simulations to the top-bin ADCP measurements showed significant improvement. The mean error disappeared and the RMSE decreased by 13% at all ADCP moorings, and by 33% at 4 of them. Comparison of simulated and real drifters was harder due to the fact that the drifter trajectories are known to exhibit chaotic behavior and to be affected by all modeling aspects. Hence we limited ourselves to the region of well defined currents and we found systematic improvement when using Stokes drift for drifters and the full wave coupling.

1. Introduction

Prediction of motion in the sea surface layer is of great practical importance but still remains a difficult problem to solve. It is of interest for both solving practical problems like oil spill prediction or search and rescue operations as is for gaining further insight into the surface ocean dynamics. In the surface layer often ignored contribution comes from the wave-current interaction. For example, assessing the importance of the current-wave coupling *Jorda et al.* [2007] found that at basin scale currents have no significant influence on the wave forecasts, whereas the wave impact on currents is much more pronounced, particularly through the modification of the wind drag coefficient. Traditionally, circulation and waves have been modelled separately, and the Adriatic Sea is not exception. *Dykes et al.* [2009], for example, ran the SWAN (Simulating Waves Nearshore) wave model in real-time, using wind inputs generated by the ALADIN 8-km atmospheric model, to provide surface waves forecast for the Adriatic Sea in support of the Dynamics of the Adriatic in Real Time (DART) field experiments. The authors report success in simulating the spatial gradients in significant wave height observed by *in situ* and remote-sensing measurements during a sirocco - southern wind event. It was also found that, compared to previous reports, use of higher-resolution wind forcing and more realistic orography reduced the underestimated 10 m wind, but did not correspondingly changed the magnitude of significant wave height. This finding in particular leaves room for further investigation of wind-wave and wave-current interactions Adriatic. *Bertotti and Cavaleri* [2009] used WAve prediction Model (WAM) to analyze the quality of predictions of wind and waves in the Adriatic Sea, highlighting the sensitivity of local wind and wave conditions to small changes in the overall meteorological patterns.

Adriatic Lagrangian measurements and related analyzes have relatively short history, primarily limited to the last two decades, but they contributed significantly to understanding its circulation. *Borzelli et al.* [1992] appear to be the first to use Lagrangian information to map northern Adriatic kinetic energy field. To that end they used positions of 5 drifting buoys satellite tracked from 25 August to 15 October 1990. Positions were typically recorded eight times per day and then nine-hour averaged; objective analysis was used to map kinetic energy on a regular 0.1 deg grid. In spite of spatial and temporal limitations of the data some known circulation features were reproduced.

Later on, *Poulain* [1999] used trajectories of satellite-tracked drifters to describe the characteristics of the surface circulation in the Adriatic Sea between December 1994 and March 1996. The inhomogeneous space and time sampling obstructed robust estimation of basin mean circulation and mesoscale eddy variations, but the circulation inferred from the drifter velocities reproduced well the known basin-wide cyclonic gyre with two embedded sub-basin cyclonic patterns, providing also a wealth of new detail information, in the Strait of Otranto in particular.

In a follow-up paper *Poulain* [2001] used data from some 200 satellite-tracked drifters released in the Adriatic Sea over a 9-year period (August 1990-July 1999) to estimate subtidal velocity statistics of the Adriatic surface circulation. Low-pass filtered drifter velocities were used to estimate Eulerian and Lagrangian statistics and derive spatial structure and the temporal variability of the surface currents, at meso- to seasonal scales. The drifter-derived mean flow confirmed the global cyclonic circulation, but also enabled numerical estimates of parameters like the width of the Western Adriatic Current (WAC) and sub-basin maximum velocities.

Castellari et al. [2001] used the same drifter data set grouped into three clusters of 5-7 drifters to study the predictability of Lagrangian particle trajectories in the Adriatic Sea. The authors employed a simple Gauss-Markov Lagrangian particle model to determine the specific scales of predictability for the Adriatic basin.

Lacotara et al. [2001] also used the December 1994 - March 1996 drifter data to analyze characteristics of drifter trajectories. The authors found that the use of Finite-Scale Lyapunov Exponent and the Lagrangian Structure Function combined with study of transport properties at spatial rather than temporal scale provides more reliable information on the relative dispersion of tracers.

Haza et al. [2007b] used the data derived from a numerical model (NCOM) set up for the Gargano Peninsula region of the Adriatic Sea to direct the launching of surface drifters during the course of the DART observational program, aiming to maximize coverage of the sampling area. To that end the Finite-Size Lyapunov Exponents (FSLE) were calculated. Model FSLE fields proved to be good indicators of regions of high relative drifter dispersion suggesting a promising way to aid real-time-directed drifter launches during field campaigns. *Ursella et al.* [2006] calculated pseudo-Eulerian and Lagrangian statistics from the low-pass-filtered velocity data derived from more than 120 satellite-tracked drifters deployed in the northern and middle Adriatic between September 2002 and December 2003. That allowed determination of the mean circulation with unprecedented high horizontal resolution, revealing maximal values of WAC mean currents, velocity variance, and kinetic energy levels, as well as autumn maxima as opposed to summer minima. The data also showed clear influence of the wind and the Po River discharge. *Veneziani et al.* [2007] investigated particle evolution as a function of initial conditions using historical drifters data with a view to aid design of field experiments. Drifter data have been also used in Eulerian modeling framework. *Taillandier et al.* [2008] adapted a mesoscale open ocean variational method to reconstruct the velocity field in the central Adriatic Sea, employing surface drifters data and output from the ROMS circulation model. The velocity reconstruction was performed using nine drifter trajectories over 45 days (from 1 October to 15 November 2002), during the DOLCEVITA field experiment minimizing the differences between observed and simulated trajectories. The results suggests that the reconstruction improved the description of the boundary current with respect to the ROMS model solution without the drifter data. *Paklar et al.* [2003] used the Princeton Ocean Model and two mesoscale numerical weather prediction models to simulate trajectories of two satellite-tracked drifters during the summertime bora episode of 22-25 June 1995. The study revealed the importance of the drag coefficient and the need to increase its numerical value in order to reproduce well the effects of the sea surface roughness and the impact of the atmospheric conditions. The need to artificially increase the drag coefficient suggests a need for re-examination of the employed air-sea interaction parameterization concept. Concerned with accurate numerical prediction of the oceanic upper layer velocity *Carniel et al.* [2009] assess the effects of vertical resolution, different vertical mixing parameterization and surface roughness values on surface layer turbulent kinetic energy injection from breaking waves. The Generic Length Scale turbulence closure formulation in the ROMS circulation model was accordingly modified. When surface roughness was allowed to depend on significant wave height the SWAN wave model was used to provide the height value. The model was applied to a realistic situation in the Adriatic Sea in which numerical drifters were released during an intense episode of bora winds (mid-February 2003) and their trajectories compared to the displacement of four satellite-tracked drifters deployed during the related field campaign. The inclusion of the wave breaking process helped improve the accuracy of the numerical simulations after, in addition to wave breaking parameterization and k-epsilon turbulence closure, an extra high value of the Charnock sea constant (56000) was applied. It is worth noting that the constant values is four orders of magnitude larger than the values commonly applied at the air side of the interface, and 40 times larger than the value suggested by *Bye* [1988].

The aim of this study has been to improve and validate the prediction of Adriatic sea surface currents taking into account the wave-current interactions and employing an up-to-date wave model and the radiation stress framework. The effort is akin to the work of *Uchiyama et al.* [2010] in which the wave-current interaction is explored employing a vortex-force formalism, ROMS circulation model [*Shchepetkin and McWilliams*, 2005] and the SWAN wave model.

The rest of the paper is organized as follows. In Section 2 the employed models and data are briefly presented. The physics of the coupling is described shortly in Section 3. Motivation for and the setup of the performed numerical experiments are laid out in Section 4. Results of the experiments are discussed in Section 5 and summarized in Section 6.

2. Models and Data

The ROMS model is a finite difference, free surface model that solves the primitive equations on curvilinear grids using the Boussinesq and hydrostatic approximations. It uses the time splitting method for time integration to resolve the numerical constraints related to the CFL criteria of gravity waves. For the advection of momentum and tracers, ROMS offers a variety of high order numerical schemes. The model used a sigma-coordinate in vertical, which implies an intrinsic error in computation of the horizontal pressure gradient, for which several possible schemes are proposed [*Shchepetkin and McWilliams*, 2003]. In accordance with the philosophy of giving the choice to the user to create the best setup for specific application, several schemes are available for bottom stress, surface stress, turbulence parametrization, boundary condition and diffusion.

The WWM-II model [*Roland*, 2008] is a wave model based on the WWM-I [*Hsu et al.*, 2005] using new numerical schemes, revised physics and more efficient algorithms. The WWM-III applies a fractional time step method according to *Tolman* [1992]. The numerical methods for the advection of wave action in geographical space are based on the Residual Distribution Schemes [*Abgrall*, 2006] and formulated using implicit or explicit time integration, where the explicit schemes are up to 2nd order in time and space while retaining monotonicity. The integration in spectral space is done as in the WaveWatch III model [*Tolman*, 1992] by application of the Ultimate Quickest approach given by *Leonard* [1991]. For nonlinear triad wave-wave interactions the Lumped Triad Approximation [*Eldeberky and Battjes*, 1995] is used, whereas the quadruplet interactions are approximated based on the Discrete Interaction Approximation according to *Hasselmann et al.* [1985]. With respect to the source terms, WWM-III includes a variety of wind input, and white capping parameterizations.

Both ROMS and WWM-III models were forced using the output from the Limited Area Model Italy (LAMI) [*Cacciami et al.*, 2002]. LAMI is a 7 km implementation of the atmospheric fully non-hydrostatic Lokal Model originally developed by the German meteorological service [*Steppeler et al.*, 2003]. The LAMI simulations of 2 m air temperature, 2 m humidity, surface air pressure, 10 m wind, longwave and shortwave radiation were available from 2002-09-18 up to 2003-06-01 and were interpolated to the ROMS ocean model grid to provide needed forcing. In order to estimate LAMI wind prediction skill we used satellite QuikSCAT scatterometer measurements along with some *in situ* measurements. QuikSCAT data provide sea surface wind field at 10 m and at 12.5 km resolution. Data were obtained from Physical Oceanography Distributed Active Archive Centre (PO.DAAC) as a Level 2B Product (http://podaac.jpl.nasa.gov/PRODUCTS/p286.html) and subsetted for the Adriatic area. *In situ* measurements used in this study were recorded at Italian gas rigs, however after visual screening and basic quality checks we used only 6 stations (Ada, AzaleaB, BarbaraC, FratelloC, Giovanna, Pennina shown at Figure 1) in our analysis. Four of those stations also had wave measurements.

The ROMS boundary forcing at the open boundary located at the Otranto strait was implemented using salinity, temperature, momentum and sea surface height interpolated from the Mediterranean Forecasting System (MFS) by *Pinardi et al.* [2003].

The current data derive from an array of RD Instruments (RDI) Workhorse Sentinel broadband ADCPs was deployed in the northern Adriatic from September 2002 to May 2003, as part of a joint research effort of several international collaborating teams [*Lee et al.*, 2005]. The moorings consisted of 16 trawl-resistant bottom-mounted ADCPs distributed along portions of 4 mooring sections with one additional ADCP off the west Istrian coast and another one mounted near the base of the meteorological tower Acqua Alta (VR1). The mooring positions are shown in Figure 1. Further details are available from *Book et al.* [2007]; *Kuzmić et al.* [2007]. During the same period total of 124 surface drifters were deployed in 188 deployments (some were recovered and redeployed more than once). They were primarily of the CODE type equipped with the standard Argos tracking and telemetry or with a Global Positioning System [*Ursella et al.*, 2006]. We used raw drifters data before any smoothing or preprocessing.

3. Wave modelling and models coupling

The theory of radiation stress was initiated by *Longuet-Higgins and Stewart* [1964] where a barotropic formulation of the stress was obtained for ocean models. A baroclinic formulation was proposed by *Mellor* [2003] but it was soon criticized [*Ardhuin et al.*, 2008a] and another formulation was proposed by *Ardhuin et al.* [2008b], which uses the Generalized Lagrangian Mean. In this formulation the model computes the quasi-Eulerian velocities and the Stokes drift is added to the advection of tracers and momentum. Wave information can also be used for modeling the sea roughness length instead of the Charnock coefficient. One classical modelization [*Burchard*, 2001; *Janssen*, 2010] is $z_0 = cH_s$ but the value of c is still opened to discussions. One classical model *Burchard* [2001]; *Janssen* [2010] is $z_0 = cH_s$ but the value of c is still opened to discussions. It is generally assumed [*Janssen*, 2010] that $c = 0.5$ but field experiment *Burchard* [2001] indicate that $c = 1.5$ is more plausible. Recently [*Saetra et al.*, 2007; *Bennis et al.*, 2011], it has been realized that improved oceanic forecasts are obtained when using surface stress obtained by integration of the wave surface stress instead of using only meteorological based formulation [*Fairall et al.*, 2003]. As a consequence we propose to use the *Ardhuin et al.* [2010] formulation of wave stress, which after integration gives the stress applied to the model.

Surface water waves are usually described by their wavenumber $\mathbf{k}$, intrinsic frequency σ and absolute frequency ω. For a given depth d and surface current $\mathbf{u}$ the dispersion relation is $\sigma^2 = gk\tanh(kd)$ with the Doppler shift relation defined as $\omega = \sigma + \mathbf{u}.\mathbf{k}$. According to the stochastic approach of modelling surface waves, they are defined with wave action $N(x, \mathbf{k})$ at a spatial position x and wave number $\mathbf{k}$. Using spectral space coordinates σ, θ for the energy we get the Wave Action Equation (WAE):

$$\frac{\partial N}{\partial t} + \nabla_x((\mathbf{c}_g + \mathbf{u}_A)N) + \frac{\partial}{\partial \omega}(\dot{\theta}N) + \frac{\partial}{\partial \theta}(\dot{\omega}N) = S_{tot}.$$

The first term in the WAE is the advection part in geographical space, the second is the frequency shifting due to currents and the last is the refraction caused by bathymetry and currents. The source term S_{tot} in the equation can be decomposed into different contributions; wind part S_{in}, the nonlinear interaction in deep and shallow water (S_{nl4} and S_{nl3}), the energy dissipation due to white capping, wave breaking and bottom friction (S_{ds}, S_{br} and S_{bf}):

$$\frac{dN}{dt} = S_{tot} = S_{in} + S_{nl3} + S_{nl4} + S_{ds} + S_{br} + S_{bf}. \tag{1}$$

By integrating the WAE one can compute the spectral wave density and thus get statistical values such as significant wave height, zero-down wave period, etc. The free surface elevation originating from the circulation model is present in the dispersion relation for waves. Following *Cavaleri et al.* [2007] the circulation velocity $\mathbf{u}_A$ is modelled by the barotropic current in shallow water and by the surface current in the deep ocean, however, modelling of the vertical sheared current effect is still missing and would require a new form in the WAE.

On the other hand effects of waves on the circulation in terms of primitive equation is more complex. The barotropic effect of waves is modelled by *Longuet-Higgins and Stewart* [1964] as a radiation stress. A baroclinic formulation was proposed by *Mellor* [2003] and later corrected by *Ardhuin et al.* [2008a]. Another formulation based on Generalized Lagrangian Mean (GLM) [*Andrews and McIntyre*, 1978] was proposed by *Ardhuin et al.* [2008b]. One should bear in mind that the obtained equation has characteristics of the quasi-Eulerian momentum as opposed to the Eulerian momentum found in the classical equations *Ardhuin* [2006].

In our approach we used the formulation of wave and circulation coupling proposed by *Bennis et al.* [2011], which are a simplified version of *Ardhuin et al.* [2008b]. Using that approach one can decompose the velocity field $\mathbf{u}$ as a sum $\mathbf{u}_{circ} + \mathbf{u}_{wave} + \mathbf{u}_{turb}$. If one assumes that wave current and circulation are statistically independent of the turbulent velocities $\mathbf{u}_{turb}$ then it is possible to make that assumption. The mean Eulerian velocity field of the wave velocity $\mathbf{u}_{wave}$ is zero, but the resulting movement of a Lagrangian particle following the current induced by the wave is non-zero, hence we have Stokes drift $\mathbf{u}_s$. If one assumes that the turbulent velocities are negligible with respect to the global circulation and are independent of the wave motions then the formalism describing combined circulation and wave movement is accomplished through the GLM.

The horizontal Stokes drift can be expressed as an integral over the wave spectrum $E(\mathbf{k}) = \sigma N(\mathbf{k})$ as

$$(u, v)_s = \int_{\mathbf{k}} \frac{E(\mathbf{k})}{2\sinh^2(kD)} \sigma \mathbf{k} \cosh(2k(z+h)) d\mathbf{k}. \quad (2)$$

If only significant wave height H_s, mean wave length L and mean direction d are available then the Stokes drift can be computed by a simpler truncation formula as

$$(u, v)_s = \frac{1}{16} H_s^2 \sigma_L \frac{2\pi}{L} \frac{\cosh(4\pi(z+h)/L)}{2\sinh^2(2\pi D/L)} (\cos d, \sin d) \tag{3}$$

with σ_L the mean frequency computed from L and the dispersion relation. On the other hand the vertical Stokes drift is computed using the non-divergence of the Stokes drift in the following way:

$$w_s(z) = -\left. u_s \right|_{z=-h} \frac{\partial h}{\partial x} - \left. v_s \right|_{z=-h} - \int_{-h}^{z} \frac{\partial u_s}{\partial x} + \frac{\partial v_s}{\partial y} dz$$

and we can define the particular derivative

$$\frac{D}{Dt} = \frac{\partial}{\partial t} + (u + u_s)\frac{\partial}{\partial x} + (v + v_s)\frac{\partial}{\partial y} + (w + w_s)\frac{\partial}{\partial z}.$$

In that approach we also need the J potential defined as

$$J = \int_{\mathbf{k}} g \frac{kE(\mathbf{k})}{\sinh(2kD)} d\mathbf{k}.$$

Using such defined Stokes drift we can write down the conservation equation for tracers like temperature or salinity

$$\frac{DT}{Dt} = C(T) + D(T) \tag{4}$$

with $C(T)$ as source or sink of tracers T and $D(T)$ the diffusion. Similarly, using additional part for the Stokes drift dynamics, the Stokes velocity $\mathbf{u}_s$ must be added to drifter trajectories when integrating in time to get their position. In that case wall boundary conditions $\mathbf{u} = 0$ should be replaced with $\mathbf{u} = -\mathbf{u}_s$ and similarly for other types of boundary conditions. The Stokes drift dynamics also enter into the part where we compute advection of momentum, where additional terms are needed to correct Eulerian only component of velocity:

$$\frac{D\mathbf{u}}{Dt} = \mathbf{F}_{pres} + \mathbf{F}_{turb} + \mathbf{F}_{cor} + \mathbf{F}_{wave} + \mathbf{F}_{bottom} + \mathbf{F}_{surf} \tag{5}$$

$\mathbf{F}_{pres}$ and $\mathbf{F}_{turb}$ are the pressure and turbulence terms respectively, while $\mathbf{F}_{cor} = f_{cor}(v + v_s, -u - u_s)$ is the Coriolis term with f_{cor} the Coriolis factor. The wave forcing term $\mathbf{F}_{wave}$ is expressed as:

$$\begin{cases} F_{wave,x} &= \frac{\partial v}{\partial x} v_s + \frac{\partial u}{\partial x} u_s - \frac{\partial J}{\partial x}, \\ F_{wave,y} &= \frac{\partial v}{\partial y} v_s + \frac{\partial u}{\partial y} u_s - \frac{\partial J}{\partial x}. \end{cases} \tag{6}$$

A wave formulation of the bottom stress $\mathbf{F}_{bottom}$ is proposed by *Bennis et al.* [2011] but in our case we will use a classical formulation. The surface stress $\mathbf{F}_{surf}$ is usually modelled according to the meteorological parameters as 10 m wind speed, 2 m air temperature, and 2 m relative humidity [*Fairall et al.*, 2003]. *Janssen* [1989] decomposed the surface stress into viscous stress, wave stress and high frequency stress. Viscous stress is generally small, wave stress is computed from the wave spectrum while *Janssen* [1989] provides a parameterization of the high frequency stress.

4. Setup used in numerical experiments

The Adriatic Sea is a narrow epicontinental basin characterized with only one open boundary at the Otranto strait through which it is connected with the Mediterranean Sea. The northern part of Adriatic Sea is a shallow (< 50 m) region while the middle and southern Adriatic have depths up to 250 m and 1200 m, respectively. Its eastern side is characterized by complex coastline with many islands and narrow, sometimes very deep straits. Complex orography surrounding the Adriatic Sea (Dinaric Alps on the east, and Apennines on the west) contribute to two dominant Adriatic winds: cold and dry cross-basin bora blowing over Dinaric passes, and warm along-basin, long-fetch southerly wind sirocco. Both winds can generate large waves.

The curvilinear Adriatic grid, used by the ROMS model, is characterized with ≈ 4 km horizontal resolution. For the WWM-III model we used an unstructured finite element mesh obtained directly from the finite difference ROMS grid by subdividing the cells. The vertical resolution within the ROMS model is composed of 20 vertical layers and uses a nonlinear stretching function in order to fit as closely as possible to the surface. However, we use a thermocline parameter of 20 m which is the right physical parameter needed to resolve physically the thermocline. Using it, we get a depth of the top most layer of the model of 5 cm in the shallowest part of the Adriatic, 33 cm in the Northern Adriatic and 54 cm in the deepest part of the Adriatic. Our other specific parameters of the ROMS model were used in the same way as in *Janeković et al.* [2010].

The ROMS model was integrated on the same 4 km grid as the one used by *Carniel et al.* [2009] but with some modifications in order to better resolve bathymetry and coastline. Furthermore the bathymetry was smoothed according to the method proposed by *Dutour Sikirić et al.* [2009]. The wave and circulation models were integrated with a 150 sec time step which was also chosen as the coupling time interval in order to minimize coupling effects between models.

For the bottom stress several parameterizations using waves are proposed by *Bennis et al.* [2011], however in our case we used the quadratic form of the drag with a constant obtained from the logarithmic profile. For the parameterization of the turbulence, we use the *gen* parameterization [*Umlauf and Burchard*, 2003]. Estimate of the surface roughness length was $z_0 = 0.5 H_s$, as proposed by *Warner et al.* [2007]; *Janssen* [2010]. Another possible estimate that we could use was by the Charnock coefficient for the sea, $z_0 = \alpha_{sea}\tau/(\rho_{sea})$. Usually the parameter α_{sea} has value of $1,400$ but higher values (i.e $14,0000$) are possible and were considered by *Carniel et al.* [2009]. The problem with those values is that even with $\alpha_{sea} = 1,400$ one gets a sea roughness length of 30 m during the bora wind, which is unrealistic and leads to a higher mixing than is found in reality [*Janssen et al.*, 2010]. For the parameterization of the surface stress we used in the wave model the formulation proposed by *Ardhuin et al.* [2010]. According to *Bennis et al.* [2011], this stress is then integrated and is used to force the circulation model. In particular this provides the sea roughness length z_0 and the friction velocity $\mathbf{u}_\star$ for the surface stress. However, we still used the COARE bulk flux formulation [*Fairall et al.*, 2003] for air-sea exchange of heat. This means that the ROMS model is using separate turbulent formulation for air-sea exchange of momentum and in particular that information from the wave model is not used for improving the heat exchange. One possible approach could be to use the unified formulation from *Janssen* [2010] or even better to couple the ROMS with a meteorological model [*Warner et al.*, 2007] but this is beyond the scope of this work. Another weakness of our formulation is the use of quadratic form for the bottom stress in coastal regions. But the main problem, appart from the forcing, is probably the insufficient resolution, which is especially problematic for the islands of the eastern coast.

In our formulation the wave model influence the circulation model in a four ways: (I) The Stokes drift computed by integration over the wave spectra is used for the computation of Lagrangian trajectories. (II) The significant wave height is used in the computation of the sea roughness length. (III) The Stokes drift dynamics is also used in the advection of tracers, momentum and as a radiation stress term inside the primitive equations. Finally

(IV) by integrating over the spectrum of the source term S_{in} in Formula 1, the correct surface stress in the primitive equation is found.

In order to quantify the relative importance of the contributions that have been implemented, we have made several experiments:

Experiment 1 is the basic ROMS model integration where we do not use any of the wave physic dynamics. For this experiment we use the Charnock relation for computing the surface roughness length. We used the value $\alpha_{sea} = 1,400$ which is the commonly used value.

Experiment 2 use the same ROMS model setup as in (1) except that we add the Stokes drift term to the Eulerian component for drifter dynamics calculations.

Experiment 3 is the same as (2) with additional formulation for surface roughness length as $z_0 = 0.5H_s$.

Experiment 4 share the same setup as (3) with the Ardhuin formulation used for the coupling wave-ocean according to Formula (4), (5) and (6).

Experiment 5 is the same as (4) except that we used the surface stress computed from the wave model rather than from COARE bulk flux formulation of *Fairall et al.* [2003].

Table 1 gives a short description of the 5 above experiments. Each of those experiment allows to estimate the relative contribution of the term introduced. Of course in Experiment 5 we are estimating cumulative effects of all contributions. This could be viewed as a problem, but as we saw later each contributions is small enough that we do not have to consider all possibilities.

5. Results and Discussion

We now turn to the discussion of the results organized around the three validation procedures. As mentioned before the validation data come from the period January - February 2003. During the period the most energetic wind with large wind speeds was the bora wind with several pronounced long lasting episodes. On the other hand, sirocco wind events were rare and usually lasted only for a day. In all our numerical experiments circulation was typical for the winter period [*Cushman-Roisin et al.*, 2001] characterized with the southward/outward colder WAC flowing along Italian coast, and the warmer northward/inward Eastern Adriatic current (EAC) flowing along the Croatian coast. During the strong and long enough bora winds well known formation of a multiple gyre current regime in the Northern Adriatic was well established [*Kuzmić et al.*, 2007]. The WAC was enhanced during the bora episodes [*Ursella et al.*, 2006] while the EAC was increased during the sirocco wind cases.

5.1. QuikSCAT validation

Quality wind input is a fundamental part of any simulation [*Bertotti and Cavaleri*, 2009] of wind/wave/ocean dynamics. In order to estimated LAMI wind forcing quality we used satellite QuikSCAT scatterometer measurements along with *in situ* measurements. QuikSCAT data provide sea surface wind field at 10 m and at 12.5 km resolution. Data were obtained from Physical Oceanography Distributed Active Archive Centre (PO.DAAC) as a Level 2B Product and subsetted for the Adriatic area. *In situ* measurements used in this study were obtained from Italian gas rigs, however after visual screening and basic quality checks we used only 6 stations (Ada, AzaleaB, BarbaraC, FratelloC, Giovanna, Pennina shown in Figure 1) in our analysis. Using the QuikSCAT data in assessing the model wind quality allowed us to estimate atmospheric model spatial errors that could not be done using only *in situ* data. QuikSCAT instrument specification gives zero bias both for the magnitude and direction and the root mean square errors (RMSE) of 2 m/s for magnitude and 20°for direction. Validation studies with *in situ* data in coastal region ($<$ 80 km) show increase in error both for magnitude (0.93 m/s $\pm$ 1.83 m/s) and for direction (4.71°$\pm$ 31.15°) [*Tang et al.*, 2004], while in the open sea it performs close to the specification. For the light winds ($<$ 3 m/s) those errors are even higher, especially for the wind direction [*Tang et al.*, 2004]. In order to compute those errors QuikSCAT L2 data were spatially interpolated onto the LAMI model grid, while the model wind data were interpolated in time onto the specific time of QuikSCAT overpass over the Adriatic Sea. Overall spatial error was derived by averaging differences between model and QuikSCAT wind magnitude and direction for each QuiksSCAT overpass. Based on the data, maps were derived for mean and standard deviation fields by using the whole time period (Figure 2).

To facilitate analysis of spatial error patterns, mean QuikSCAT wind magnitude and direction (Figure 3) were derived. Finally, statistical estimates for bias were derived as LAMI minus QuikSCAT or *in situ* values, showing that LAMI underestimate wind magnitude (-0.56 m/s) when compared against QuikSCAT measurements (total number of samples used in the analysis was 299125) and overestimate it (0.82 m/s) when compared to the *in situ* measurements (total number of used records was 2315). Standard deviations are similar for both QuikSCAT and *in situ* data ($\approx$ 2.9 m/s). Overall direction bias is positive for both QuikSCAT and *in situ* data (9.98°and 5.12°), with standard deviations smaller for QuikSCAT (37.20°vs. 58.62°for *in situ*).

Overall spatial wind magnitude differences (Figure 2.a) are highly correlated with areas of higher or lower wind speeds (Figure 3) and are in range between -3 and 3 m/s. Highest positive errors are correlated with lower overall mean wind magnitude, except in the southern Adriatic, where this error is correlated with the higher mean wind magnitude. Underestimation of the model wind magnitude fields (negative bias) is correlated with the higher mean wind magnitudes (i.e. Kvarner and Sibenik regions strongly under the influence of the bora wind). Wind magnitude standard deviation ranges from 3 to 5 m/s with the highest values in the middle and central Adriatic. Modelled wind direction bias is the highest for the NNE winds ($\approx 35°$) where the bias values are exceeding 15°, while for other wind directions bias is less than 10°. Standard deviation is relatively uniform around the whole Adriatic ($\approx 30°$), with the higher values around the western Adriatic coast ($\approx 50°$) and around the SE Adriatic coast ($\approx 70°$). Scatter density plots of the LAMI model wind magnitude and direction compared to QuikSCAT (Figure 4 a,b) and *in situ* ones (Figure 4 c,d) shows good correlation (0.7) except for the *in situ* wind direction where the correlation is ≈ 0.4.

We used two periods of strong wind crucial for the evolution of the modelling system skill. The first episode from 7 till 13 of January 2003, characterized by strong bora wind blowing across the Kvarner Basin providing a good basis for our comparison. We also select another bora episode from 9 to 15 February, which is slightly weaker but also occurs over Senj and Dubrovnik. The mean winds for both periods are plotted on Figure 5.

In Figures 6 and 7 we give the time series of significant wave height for both periods using experiment 5. The forecasted significant wave heights vary very little between experiments 2 to 5. It appears that that the wave model give generally satisfying results except for the peaks that it tends to overestimate. One explanation for this phenomenon is that the measurement were not done in optimal oceanographic conditions, but instead on gas rigs that tend to dissipate the waves. Secondly it appears on Figure 4 that while the LAMI model generally underestimate wind speeds, it tend to overestimate them in the range 15-20 m/s.

5.2. ADCP comparison

The ADCPs moorings were predominantly located in the northern Adriatic, providing valuable observations of the currents throughout the most of the water column. An ADCP by design measures currents using the Doppler effect, sampling the sea at a sphere lobe and should not be considered a single point measurement like e.g. the classical Aanderaa current meters. An ADCP provides velocity averaged over the sampled volume from, in our case 4 beams. We limit our model to ADCP comparison only to the top-most measurement of surface velocity since we are interested foremost in drifter movements and surface wave/wind induced dynamics, the most pronounced in the surface bin. Model output and ADCP were detided using harmonic K1, M2, S2, N2, K2, O1 and P1.

Result of Root Mean Square Error (RMSE) and Mean Error (ME) are indicated in Table 2 for the magnitude of the top-most current. For that comparison we interpolated model values at to the exact geo-locations of ADCPs as well at the same depth of the top-most ADCP bin cell depth. The result shows that setting the roughness length (our Experiment 3) has limited effect on the final results but at the same time that the Ardhuin formulation of radiation stress (our Experiment 2) led to improvement for almost all ADCP measurements. Also, using the surface stress from the wave model (our Experiment 5) led to no significant changes in the statistical sense. However, time series show that there is a small reduction in the current magnitude that appears to be in the right direction (Figure 8). Relatively poor results we obtained for ADCPs VR6, SS2 and SS4 which are located near the coast and for which resolution of the model is not adequate. However for station KB1, which is in the Kvarner Bay channel and is directly exposed for the case of strong bora the results are better when using waves formulations (Experiment 5).

In Figure 9 we show the mean surface current for this period and 4 experiments. The result shows that, in general, when using the formulation $z_0 = 0.5H_s$ for the roughness length there is a small net decrease of the magnitude of the surface current. This is especially true for the south tip of Istria and entrance of the Kvarner Bay, where one finds a 15% decrease for the surface mean current error. When using Ardhuin formulation we found a larger reduction in surface current magnitude in the same regions. Using the surface stress from the wave model led a much smaller reduction in surface current magnitude. Similar reductions of average current are apparent near the Italian coast and the Venice lagoon. In Figure 10 we show the mean free surface for the period and experiment 1, 3, 4 and 5. The result differ very little between experiments, which is expected. The largest discrepancy occurs near the Italian coast where the use of Ardhuin formulation and surface stress from wave lead to a 4 cm reduction of the free surface, which is coherent with the decrease in surface current velocity.

In Figure 8 we showed the magnitude of surface currents for the period of strong bora wind from 2003-01-07 till 2003-01-13. The result for the rest of the ADCPs are in a way consistent showing a small but positive improvement of the result where observations are not made in the regions with strong wind/wave dynamics. This is due to the fact that when one uses a roughness derived from frictional velocity and Charnock parameter (see

Figure 11) then the roughness length can become larger than what is physical. In our study and experiment 3 we also used the value $z_0 = H_s$ and found that the result are only slightly changed. The largest difference occurs when one uses full Ardhuin formulation for the radiation stress inside the Ocean model. In that case we got that ME for all ADCPs was close to 0 and a 14% improvement for the RMSE. The improvement is particularly sensible for ADCPs at VR1, KB1 and CP3 for which we find a 33% decrease in error. The only ADCP for which we have decrease of the quality of the results are SS2, SS4 and SS6. For SS2 and SS4 this can be interpreted by the fact that those ADCP are relatively near to the coast and are capturing part of WAC not represented by the model dynamics correctly. Also the bathymetry gradient is relatively large near those stations which is known to induce error in the horizontal pressure gradient calculation. The decrease in the magnitude of the surface currents is also observed near the Eastern Italian coast and the Venice Lagoon. The use of the surface stress from the wave model, as in our experiment 5, did not produced significant effect on the overall result as one could expect. This may be explained by the fact that the Bulk Flux formulation is relatively adequate for the Adriatic Sea and that well tested empirical formula can still give a fairly very good results. Note that in certain cases even when waves were modelled according to a 1 node wave model [*Saetra et al.*, 2007], i.e. no spatial advection, one can get improved results.

When analyzing the situation for the period 9th till 15th of February 2003, shown in Table 3 and Figure 12 we found significant differences. As before, we found that the mean error disappears and the RMSE decreases, this time by $\approx 25\%$ for all ADCPs. For majority of ADCPs, the result of all experiments gives similar small error. On the other hand, for ADCPs CP3, KB1, SS2 and SS4 for which experiment 1 has large errors, we saw $\approx 30\%$ improvements for the same experiment 4 and 5.

5.3. Drifter comparison

An important aspect of our modeling is the use of Stokes drift obtained by integration over the spectrum by formula (2) as opposed to the truncation formula (3). In Figure 13 both surface Stokes drifts are shown for mentioned approaches and a typical wave spectrum. It is apparent that the truncation formula led to higher Stokes drift magnitude that are not typical. Possible explanation for that is that it does not account for the directional spreading of the wave spectrum. That method should be used when no other possibility are available but one should be aware that it can overestimate by a factor of 2 the Stokes drift in a region where wind/wave dynamics is important. In our model to drifter comparison we selected only GPS based drifters and we used raw drifter data before any pre-processing manipulations. For the period of January - February 2003, this gave us 10 usable drifters trajectories.

If a drifter is placed in a region in between two gyres (similar like bifurcation point) with the model predicting the initial position at slightly different position then it will not be able to predict accurately the rest of the trajectory. This is due to the well known fact that the drifter exhibits a chaotic behavior in most oceanographic applications. This dispersion is estimated by the Finite Scale Lyapunov Exponent. One example of dispersion with 20 drifter within 2 km is shown in Figure 14 for 3 cases. It shows that while the spreading of trajectories varies from case to case it is relatively small when the drifter are in significant currents.

In order to limit the dependency on the initial position, we shift the starting point of the drifter in time, i.e. to a real drifter we associate many virtual drifters each separated by 6 hours from their starting point. We found out that the region of high chaoticity are the regions of Po river plume, and the coastal regions on the Croatian side between Zadar and Trieste. This could be explained by the fact that those regions are characterized by varying currents. So, we limit ourselves to the trajectories where the current is well defined and for which we can expect the result to be significant for the estimation of the relative effects of the parameterizations.

As a consequence we investigate the behavior of drifters only in the Istrian bora jets domain and near the Italian coastline in the Northern Adriatic. Both those domains are exposed to large wave that magnify the importance of the coupling. Furthermore currents are relatively large that make the comparison relatively significant. Four drifter trajectories lasting 5 days are plotted in Figure 15 together with the virtual trajectories of the 5 experiments. For all those drifters, the significant wave height was larger than 1 m. We saw that experiment 4 differ significantly from experiment 5 which shows that despite the smallness of the impact for ADCP comparison, the impact is much larger for the drifters. More generally, the fact that all trajectories are significantly different serves to illustrate the chaoticity of drifter trajectories in oceanic modelling. All 4 cases considered show a positive and significant impact of the use of Stokes drift in computing the evolution of drifters. The specification of the roughness length from the wave model in experiment 3 gives improvement only for Drifter (b). However the use of surface stress yield from the wave model yield better results for (a) and (b). This can be explained by the fact that experiment 4 and 5 saw decrease of Eulerian surface currents that compensate for the increase due to the added Stokes drift. For (c) and (d), which are near the Italian coast, the use of Ardhuin formulation and surface stress from the wave model do not yield additional improvement but the results are still better than experiment 1 and one has to bear in mind that we saw in Table 2 and 3 that the ADCP SS2 and SS4 located near those drifters had larger RMSE.

6. Conclusions

In this paper we have explored the impact of combined circulation and waves modeling on predicting the near-surface motions in (primarily northern) Adriatic Sea. To that end the latest concepts in physics of spectral wave models were used to close the momentum balance in the surface boundary layer. To force the ROMS and WWM-III models and to assess their modeling skill parts of an existing database of observational and simulation data were used. In particular, focusing on the period January - February 2003, the LAMI output was used to force the ROMS and WWM-III models, *in situ* and scatterometer wind data to validate the wind forcing, and ADCP and drifter data to assess the skill of the ROMS+WWM-III system.

The implementation of the two-way coupled ROMS and WWM-III models was used as a computational platform for five numerical experiments. In the first experiment, design to provide the baseline, no coupling to the wave model is implemented and the surface stress is modelled assuming commonly used value of $\alpha_{sea} = 1,400$, although some other values have been proposed (for example $\alpha_{sea} = 18,500$ *Burchard* [2001]; *Craig and Banner* [1994]). In the second experiment the wave model was statically linked to ROMS and used to calculate the Stokes drift as an integral over the wave spectrum. The Stokes drift was then used only to correct the motion of simulated drifters. It appears from our simulations that it is indispensable to compute the Stokes drift from the wave spectrum and not from a truncation formula. In the next experiment the previous experiment was modified to include roughness length dependence on the significant wave height. This change alone had rather limited impact on the simulation. In the fourth experiment the wave stress was also included in the equations of motion. The comparison of simulations to the top-bin ADCP measurements shows significant improvement when using this experiment model setup. The mean error disappears and the RMSE decreases by 13% at all ADCP moorings and by 33% at 4 of them. These results are further improved when in addition to wave stress the wind stress is made wave-depended, instead of the usual bulk flux dependence (the fifth experiment). Comparison of results for drifters is harder due to the fact that drifter trajectories are known to be chaotic and to be affected by all aspects of the modelization. Moreover, the movement of the drifters is depended on small scale local processes that would actually require a more sophisticated model of the drifter in contrast to passive tracer as used in the modelling. However, in fifth experiment we found systematic improvements when using Stokes drift for drifters and the formulation of wave coupling.

Acknowledgments. This work has been supported by the Croatian Ministry of Science, Education and Sport under contract 098-0982705-2707. Thanks to Rich Signell for preparing netCDF files with the meteorological data from Italian gas rigs, and Jacopo Chigiatto for providing LAMI data. We are thankful to Peter Janssen for useful discussions of the wave physics.

References

Abgrall, R. (2006) Residual distribution schemes: current status and future trends, *Comput. Fluids*, 35(7), 641–669, doi:10.1016/j.compfluid.2005.01.007.

Andrews, D. G., and M. E. McIntyre (1978), An exact theory of nonlinear waves on a Lagrangian mean flow, *J. Fluid. Mech.*, 89(DEC), 609–646.

Ardhuin, F., E. Rogers, A. V. Babanin, J. F. Filipot, R. Magne, A. Roland, A. van der Westhuysen, P. Queffeulou, J. M. Lefevre, L. Aouf, and F. Collard (2010), Semiempirical dissipation source functions for ocean waves. Part I: Definition, Calibration, and Validation, *J. Phys. Oceanogr.*, 40(9), 1917–1941, doi:10.1175/2010JPO4324.1.

Ardhuin, F., A. D. Jenkins, and K. A. Bellibassakis (2008), Comments on "the three-dimensional current and surface wave equations", *J. Phys. Oceanogr.*, 38(6), 1340–1350, doi:10.1175/2007JPO3670.1.

Ardhuin, F., N. Rascle, and K. A. Belibassakis (2008), Explicit wave averaged primitive equations using a generalized lagrangian mean, *Ocean Model.*, 20(1), 35–60, doi:10.1016/j.ocemod.2007.07.001.

Ardhuin, F., L. Marie, N. Rascle, P. Forget, and A. Roland (2009), Observation and Estimation of Lagrangian, Stokes, and Eulerian Currents Induced by Wind and Waves at the Sea Surface, *J. Phys. Oceanogr.*, 39(11), 2820–2838, doi:10.1175/2009JPO4169.1.

Ardhuin, F. (2009), Momentum balance in shoaling gravity waves: comments on "Shoaling surface gravity waves cause a force and a torque on the bottom" by K. E. Kenyon, *J. Oceanogr.*, 62(6), 917–922, doi:10.1007/s10872-006-0109-8.

Bennis, A.-C., F. Ardhuin, and F. Dumas (2010), On the coupling of wave and three-dimensional circulation models: Choice of theoretical framework, practical implementation and adiabatic tests, *Ocean Model.*, 40(3-4), 260–272, 10.1016/j.ocemod.2011.09.003.

Bertotti, L., and L. Cavaleri (2009), Wind and wave predictions in the Adriatic Sea, *J. Marine Syst.*, 78(S), 227–234, doi:10.1016/j.jmarsys.2009.01.018.

Book, J. W., R. P. Signell, and H. Perkins (2007), Measurements of storm and nonstorm circulation in the Northern Adriatic: October 2002 through April 2003, *J. Geophys. Res.*, 11(C11), C11S92, doi:10.1029/2006JC003556.

Borzelli, G., R. Ligi, and E. Ferulano (1992), Surface circulation in the northern Adriatic as revealed by a drifter experiment, *Nuovo Cimento C*, 15(3), 265–274, doi:10.1007/BF02533651.

Burchard, H. (2001), Simulating the Wave-Enhanced Layer under breaking surface waves with two-Equation Turbulence Models, *J. Phys. Oceanogr.*, 31(11), 3133–3145, doi:10.1175/1520-0485(2001)031¡3133:STWELU¿2.0.CO;2.

Bye, J. A. T. (1988), The coupling of wave drift and wind velocity profiles, *J. Mar. Res.*, 46(3), 457–472, doi:10.1357/002224088785113559.

Cacciamani, C., P. Emiliani, M. Ferri, and E. Minguzzi (2002), In: Doms G., Shatter, U. (Eds.), High resolution verification of hydrostatic and Non-Hydrostatic LAM Precipitation Forecasts in Italy, *COSMO Newletter* (vol. 2 Deutscher WetterDienst (DWD), Offenbach), pp. 176–186.

Carniel, S., J. C. Warner, J. Chiggiato, and S. Mauro (2009), Investigating the impact of surface wave breaking on modeling the trajectories of drifters in the northern Adriatic Sea during a wind-storm event, *Ocean Model.*, 30(2-3), 225–239, doi:10.1016/j.ocemod.2009.07.001.

Castellari, S., A.Griffa, T. M. Ozgokmen, and P. M. Poulain (2001), Prediction of particle trajectories in the Adriatic Sea using Lagrangian data assimilation, *J. Marine Syst.*, 29(1-4), 33–50, doi:10.1016/S0924-7963(01)00008-2.

Cavaleri, L., J. H. G. M. Alves, F. Ardhuin, A. V. Babanin, M. Banner, K. A. Belibassakis, M. Benoit, M. Donelan, J. Groeneweg, T. H. C. Herbers, P. Hwang, P. A. E. M. Janssen, T. Janssen, I. V. Lavrenov, R. Magne, J. Monbaliu, M. Onorato, V. Polnikov, D. Resio, W. E. Rogers, A. Sheremet, J. Mc. Smith, H. L. Tolman, G. van Vledder, J. Wolf, and I. Young (2007), Wave modelling - the state of the art, *Prog. Oceanogr.*, 75(4), 503–674, doi:10.1016/j.pocean.2007.05.00.

Craig, P. D., and M. L. Banner (1994), Modeling wave-enhanced turbulence in the ocean surface layer, *J. Phys. Oceanogr.*, 24(12), 2546–2559, doi:10.1175/1520-0485(1994)024¡2546:MWETIT¿2.0.CO;2.

Cushman-Roisin, B., M. Gačić, P.-M. Poulain, and A. Ategiani (2001), *Physical Oceanography of the Adriatic Sea: Past, Present and Future*, Kluwer Academic Publishers, Dordrecht, 304 pp.

Dutour Sikirić, M. A., I. Janeković, and M. Kuzmić (2009), A new approach to bathymetry smoothing in sigma-coordinate ocean models, *Ocean Modell.*, 29(2), 128–136, doi:10.1016/j.ocemod.2009.03.009.

Dykes, J. D., D. W. Wang, and J. W. Book (2009), An evaluation of a high-resolution operational wave forecasting system in the Adriatic Sea, *J. Marine Syst.*, 78(SI), S255–S271, doi:10.1016/j.jmarsys.2009.01.027.

Eldeberky, Y., and J. A. Battjes (1995), Parameterization of triad interactions in wave energy models, Proceedings Coastal Dynamics Conference 95, Gdansk, Poland, 140–

148.

Fairall, C. W., E. F. Bradley, J. E. Hare, A. A. Grachev, and J. B. Edson (2003), Bulk parameterization of air-sea fluxes: updates and verification for the Coare algorithm, *J. Climate*, 16(4), 571–591, doi:10.1175/1520-0442(2003)016¡0571:BPOASF¿2.0.CO;2.

Falco, P, A. Griffa, P.-M. Poulain, E. Zambianchi (2000), Transport Properties in the Adriatic Sea as Deduced from Drifter Data, *J. Phys. Oceanogr.*, 30(8), 2055–2071, DOI: 10.1175/1520-0485(2000)030¡2055:TPITAS¿2.0.CO;2.

Hasselmann, S., K. Hasselmann, J. H. Allender, and T. P. Barnett (1985), Computations and parameterizations of the nonlinear energy transfer in a gravity-wave spectrum. Part II: Parameterizations of the nonlinear Energy Transfer for Application in Wave Models, *J. Phys. Oceanogr.*, 15(11), 1378–1391, doi:10.1175/1520-0485(1985)015¡1378:CAPOTN¿2.0.CO;2.

Haza, A. C., L. I. Piterbarg, P. Martin, T. M. Ozgokmen, A. Griffa (2007a), A Lagrangian subgridscale model for particle transport improvement and application in the Adriatic Sea using the Navy Coastal Ocean Model, *Ocean Model.*, 17(1), 68–91, doi:10.1016/j.ocemod.2006.10.004.

Haza, A. C, A. Griffa, P. Martin, A. Molcard, T.-M. Ozgokmen, A. C. Poj, R. Barbanti, J. W. Book, P.-M. Poulain, M. Rixen, and P. Zanasca (2007b), Model-based directed drifter launches in the Adriatic Sea: Results from the DART experiment, *Geophys. Res. Lett.*, 34(10), L10605, doi:10.1029/2007GL029634.

Hsu, T. W., S.-H. Ou, and J.-M. Liau (2005), Hindcasting nearshore wind waves using a FEM code for SWAN, *Coast. Eng.*, 52(2), 177–195, doi:10.1016/j.coastaleng.2004.11.005.

Janeković, I., M. A. Dutour Sikirić, I. Tomazić, and M. Kuzmić (2010), Hindcasting the Adriatic Sea surface temperature and salinity: A recent modeling experience, *Geofizika*, 27(2), 85–100.

Janssen, P. A. E. M. (1989), Wave-induced Stress and the Drag of Air Flow over Sea Waves, *J. Phys. Oceanogr.*, 19(6), 745–754, doi:10.1175/1520-0485(1989)019¡0745:WISATD¿2.0.CO;2.

Janssen, P. A. E. M. (2010), Ocean wave effects on the daily cycle of SST, *ECMWF Tech. Mem. 634*, Reading, United Kingdom.

Jorda, G, R. Bolanos, M. Espino, and A. Sanchez-Arcilla (2007), Assessment of the importance of the current-wave coupling in the shelf ocean forecasts, *Ocean Sci.*, 3(3), 345–362, doi:10.5194/osd-3-1825-2006.

Kuzmić, M., I. Janeković, J. W. Book, P. J. Martin, and J.D. Doyle (2007), Modeling the northern Adriatic double-gyre response to intense bora wind: A revisit, *J. Geophys. Res.*, 111(C3), C03S13, doi:10.1029/2005JC003377.

Lacorata, G, E. Aurell, and A. Vulpiani (2001), Drifter dispersion in the Adriatic Sea: Lagrangian data and chaotic model, *Ann. Geophys.*, 19(1), 121–129, doi:10.5194/angeo-19-121-2001.

Lee, C. M., F. Askari, J. Book, S. Carniel, B. Cushman-Roisin, C. Dorman, J. Doyle, P. Flament, C. K. Harris, B. H. Jones, M. Kuzmić, P. Martin, A. Ogston, M. Orlić, H. Perkins, P.-M. Poulain, J. Pullen, A. Russo, C. Sherwood, R.P. Signell, and D. Thaler Detweiler (2005), Northern Adriatic Response to a Wintertime Bora Wind Event, *Eos Trans. AGU*, 86(16), 157–168, doi:10.1029/2005EO160001.

Leonard, B. P. (1991), The ultimate conservative difference scheme applied to unsteady one-dimensional advection, *Comput. Method. Appl. M.*, 88(1), 17–74, doi:10.5194/angeo-19-121-2001.

Longuet-Higgins, M. S., and R. W. Stewart (1964), Radiation stresses in water waves; a physical discussion with applications, *Deep-Sea Res.*, 11(4), 529–562, doi:10.1016/0011-7471(64)90001-4.

Maurizi, A, A. Griffa, P.-M. Poulain, and F. Tampieri (2004), Lagrangian turbulence in the Adriatic Sea as computed from drifter data: Effects of inhomogeneity and nonstationarity, *J. Geophys. Res.*, 109(C4), C04010, doi:10.1029/2003JC002119.

Mellor, G. L. (2003), The three-dimensional current and surface wave equations, *J. Phys. Oceanogr.*, 33(9), 1978–1989, doi:10.1175/JPO2827.1.

Ozgokmen, T. M., A. Griffa, L. I. Piterbarg, and A. Mariano (2000), On the predictability of Lagrangian trajectories in the ocean, *J. Atmos. Ocean Tech.*, 17(3), 366–383, doi:10.1175/1520-0426(2000)017¡0366:OTPOLT¿2.0.CO;2.

Paklar, G. B., N. Zagar, M. Zagar Mark, R. Vellore, D. Koracin, P.-M. Poulain, M. Orlić, I. Vilibić, and V. Dadić (2008), Modeling the trajectories of satellite-tracked drifters in the Adriatic Sea during a summertime bora event, *J. Geophys. Res.*, 113(C11), C11S04, doi:10.1029/2007JC004536.

Perkins, H. T., F. de Strobel, and L. Gualdesi (2000), The Barney Sentinel Trawl-resistant ADCP bottom mount: Design, testing, and application, *IEEE J. Oceanic Eng.*, 25(4), 430–436, doi:10.1109/48.895350.

Pinardi, N., I. Allen, E. Demirov, P. De Mey, G. Korres, A. Lascaratos, P. Y. Le Traon, C. Maillard, G. Manzella, and C. Tziavos (2003), The Mediterranean ocean forecasting system: first phase of implementation (1998-2001), *Ann. Geophys.*, 21(1), 3–20, doi:10.5194/angeo-21-3-2003.

Poulain, P.-M. (1999), Drifter observations of surface circulation in the Adriatic Sea between December 1994 and March 1996, *J. Marine Syst.*, 20(1-4), 231–253, doi:10.1016/S0924-7963(98)00084-0.

Poulain, P.-M. (2001), Adriatic Sea surface circulation as derived from drifter data between 1990 and 1999, *J. Marine Syst.*, 29(1-4), 3–32, doi:10.1016/S0924-7963(01)00007-0.

Raicich, F. (1994), Notes on the flow rates of the Adriatic rivers, *Tech. Rep. RF 02/94*, 8pp., CNR, Ist Sper Talassografico, Trieste, Italy.

Roland, A. (2008), Development of the WWM II - Spectral wave modelling on unstructured meshes, PhD thesis, Dep. of Hydraulic Eng., Univ. of Darmstadt, Germany.

Saetra, O., J. Albretsen, and P. A. E. M. Janssen (2007), Sea-state dependent momentum fluxes for ocean modeling, *J. Phys. Oceanogr.*, 37(11), 2714–2725, doi:10.1175/2007JPO3582.1.

Shchepetkin, A. F., and J. C. McWilliams (2003), A method for computing horizontal pressure-gradient force in an oceanic model with a non-aligned vertical coordinate, *J. Geophys. Res.*, 108(C3), 3090, doi:10.1029/2001JC001047.

Shchepetkin, A. F. and J. C. McWilliams (2005), The regional ocean modeling system (ROMS): A split-explicit, free-surface, topography-following-coordinate oceanic model, *Ocean Model.*, 9(4), 347–404, doi:10.1016/j.ocemod.2004.08.002.

Steppeler, J., G. Doms, U. Schattler, H. W. Bitzer, A. Gassmann, U. Damrath, and G. Gregoric (2003), Meso-gamma scale forecasts using the nonhydrostatic model LM, *Meteorol. Atmos. Phy.*, 82(1-4), 75–96, doi:10.1007/s00703-001-0592-9.

Taillandier, V., A. Griffa, P.-M. Poulain, R. Signell, J. Chiggiato, and A. Carniel (2008), Variational analysis of drifter positions and model outputs for the reconstruction of surface currents in the central Adriatic during fall 2002, *J. Geophys. Res.*, 113(C4), C04004, doi:10.1029/2007JC004148.

Takaya, Y., J. R. Bidlot. A. C. M. Beljaars, P. A. E. M. Janssen (2010), Refinements to a prognostic scheme of skin sea surface temperature, *J. Geophys. Res.*, 115(C6), C06009, doi:10.1029/2009JC005985.

Tang, W., W. T. Liu, and B. W. Stiles (2004), Evaluation of high-resolution ocean surface vector winds measured by QuikSCAT scatterometer in coastal regions, *IEEE T. Geosci. Remote*, 42(8), 1762–1769, doi:10.1109/TGRS.2004.831685.

Terray, E. A., M. A. Donelan, Y. C. Agrawal, W. M. Drennan, K. K. Kahma, A. J. Williams, P. A. Hwang, and S. A. Kitaigorodskii (1996), Estimates of kinetic energy dissipation under breaking waves, *J. Phys. Oceanogr.*, 26(5), 792–807, doi:10.1175/1520-0485(1996)026¡0792:EOKEDU¿2.0.CO;2.

Tolman, H. J. (1992), Effects of numerics on the physics in a third-generation wind-wave model, *J. Phys. Oceanogr.*, 22(10), 1095–1111, doi:10.1175/1520-0485(1992)022¡1095:EONOTP¿2.0.CO;2.

Uchiyama, Y., J. C. McWilliams, and A. F. Shchepetkin (2010), Wave-current interaction in an oceanic circulation model with a vortex-force formalism: Application to the surf zone, *Ocean Model.*, 34(1-2), 16–35, doi:10.1016/j.ocemod.2010.04.002.

Umlauf, L., and H. Burchard (2003), A generic length-scale equation for geophysical turbulence models, *J. Mar. Res.*, 61(2), 235–265, doi:10.1357/002224003322005087.

Ursella, L., P.-M. Poulain, and R. P. Signell (2006), Surface drifter derived circulation in the northern and middle Adriatic Sea: Response to wind regime and season, *J. Geophys. Res.*, 112(C3), C03S04, doi:10.1029/2005JC003177.

Veneziani, M., A. Griffa, and P.-M. Poulain (2007), Historical Drifter Data and Statistical Prediction of Particle Motion: A Case Study in the Central Adriatic Sea, *J. Atmos. Oceanic. Tech.*, 24(2), 235–254, doi:10.1175/JTECH1969.1.

Warner, J. C., B. Armstrong, R. He, and J. B. Zambon (2010), Development of a Coupled-Ocean-Atmosphere-Wave-Sediment-Transport (COAWST) Modeling System, *Ocean Model.*, 35(3), 230–244, doi:10.1016/j.ocemod.2010.07.010.

Warner, J. C., C. R. Sherwood, R. P. Signell, C. K. Harris, and H. G. Arango (2008), Development of a three-dimensional, regional, coupled wave, current, and sediment-transport model, *Comput. Geosci.*, 34(10), 1284–1306, doi:10.1016/j.cageo.2008.02.012.

Figure 1. Positions of the ADCP stations and gas rigs used for comparison with model results

Figure 2. Spatial error fields of the difference between LAMI and QuikSCAT data. A) Wind magnitude bias, b) wind magnitude standard deviation, c) wind direction bias and d) wind direction standard deviation.

Figure 3. Mean QuikSCAT wind magnitude and direction for the period of January - February 2003

Figure 4. Scatter density plots between LAMI and a) QuikSCAT wind magnitude data, b) QuikSCAT wind direction, c) in situ wind magnitude and d) in situ wind direction

Figure 5. Mean winds for the periods of 7 to 13 january (a) and 9 to 15 february (b)

Figure 6. Significant wave height measured at the station Ada, BarbaraC, Giovanna and Pennina for the period 07-01-2003 to 13-01-2003 in black. In red hindcasted significant wave height from experiment 5 are represented

Figure 7. Significant wave height measured at the station Ada, BarbaraC, Giovanna and Pennina for the period 09-02-2003 to 15-02-2003 in black. In red hindcasted significant wave height by experiment 5 are represented

Figure 8. Detided current magnitude measured by ADCP in the top-most layer and experiments 1, 3, 4 and 5 for 4 ADCP for the period 07-01-2003 to 13-01-2003. The Experiments are described in Section 4 and Table 1

Figure 9. Mean surface current magnitude for the period 07-01-2003 to 13-01-2003 for experiment 1 (a), 3 (b), 4 (c) and 5 (d). The Experiments are described in Section 4 and Table 1

Figure 10. Mean free surface for the period 07-01-2003 to 13-01-2003 for experiment 1 (a), 3 (b), 4 (c) and 5 (d). The Experiments are described in Section 4 and Table 1

Figure 11. Scatter plot of Charnock coefficient obtained from the bulk formulation of *Fairall et al.* [2003] and the integration of wave stress

Figure 12. Current magnitude measured by ADCP in the top-most layer and experiment 1, 3, 4 and 5 for 4 ADCP for the period 09-02-2003 to 15-02-2003. The Experiments are described in Section 4 and Table 1

Figure 13. Stokes drift computed from a) truncation formula (3) and b) integration of wave spectra from formula (2)

Figure 14. Spreading of drifter trajectories from initial positions at 3 different times for the same drifter. 20 drifter were released within 2 km of the initial position of the real drifter.

Figure 15. 4 Trajectories of drifters with red the real trajectory, black the trajectory of experiment 1, dark blue the trajectory of experiment 2, light blue the trajectory of experiment 3, yellow the trajectory of experiment 4 and pink the trajectory of experiment 5. By H_s we denote the mean significant wave height over the trajectory of the drifter as forecasted in experiment 5. The Experiments are described in Section 4 and Table 1

Table 1. Brief description of the 5 experiments done in this paper

	run 1	run 2	run 3	run 4	run 5
Drifter velocity	$\mathbf{u}$	$\mathbf{u}+\mathbf{u}_s$	$\mathbf{u}+\mathbf{u}_s$	$\mathbf{u}+\mathbf{u}_s$	$\mathbf{u}+\mathbf{u}_s$
roughness length	$z_0=\alpha_{sea}\tau/(\rho_{sea})$	$z_0=\alpha_{sea}\tau/(\rho_{sea})$	$z_0=0.5H_s$	$z_0=0.5H_s$	$z_0=0.5H_s$
radiation stress	none	none	none	Formula (4), (5) and (6)	Formula (4), (5) and (6)
surface stress	bulk	bulk	bulk	bulk	wave

Table 2. Bathymetry and depth of topmost layer of ADCP used and result of comparison of model results with measurement for the period 07-01-2003 to 13-01-2003. The Experiments are described in Section 4 and Table 1

	run1	run3	run4	run5	Bathymetry	Depth top most layer
VR1 RMSE	0.16	0.15	0.10	0.10	15.20	-1.71
ME	-0.10	-0.09	0.01	0.00		
VR2 RMSE	0.16	0.14	0.08	0.08	21.40	-2.43
ME	-0.12	-0.10	-0.01	-0.01		
VR4 RMSE	0.11	0.11	0.10	0.10	30.60	-2.55
ME	-0.04	-0.04	-0.02	-0.02		
VR5 RMSE	0.05	0.05	0.04	0.04	31.20	-3.22
ME	-0.01	-0.01	0.00	0.01		
VR6 RMSE	0.06	0.06	0.06	0.05	29.60	-2.56
ME	-0.03	-0.03	-0.03	-0.02		
SS2 RMSE	0.25	0.25	0.29	0.30	25.40	-1.90
ME	0.14	0.14	0.25	0.25		
SS4 RMSE	0.14	0.15	0.16	0.16	45.30	-4.03
ME	0.02	0.02	0.09	0.09		
SS5 RMSE	0.10	0.09	0.08	0.08	57.20	-4.50
ME	0.01	0.01	0.02	0.02		
SS6 RMSE	0.07	0.07	0.08	0.08	66.30	-5.41
ME	-0.01	-0.01	-0.01	-0.01		
SS8 RMSE	0.16	0.16	0.16	0.15	64.70	-5.08
ME	-0.08	-0.08	-0.07	-0.06		
SS9 RMSE	0.11	0.10	0.10	0.10	58.50	-4.39
ME	-0.03	-0.03	-0.02	-0.01		
CP3 RMSE	0.16	0.15	0.09	0.09	38.40	-3.38
ME	-0.13	-0.12	-0.05	-0.05		
KB1 RMSE	0.34	0.33	0.22	0.22	48.00	-3.85
ME	-0.29	-0.27	-0.17	-0.17		
Total RMSE	0.16	0.16	0.14	0.14		
ME	-0.05	-0.05	-0.00	0.00		

Table 3. Bathymetry and depth of topmost layer of ADCP used and result of comparison of model results with measurement for the period 09-02-2003 to 15-02-2003. The Experiments are described in Section 4 and Table 1

	run1	run3	run4	run5	Bathymetry	Depth top most layer
VR1 RMSE	0.07	0.06	0.07	0.07	15.20	-1.71
ME	-0.02	-0.01	0.05	0.05		
VR2 RMSE	0.04	0.04	0.06	0.06	21.40	-2.43
ME	-0.01	0.00	0.04	0.04		
VR4 RMSE	0.04	0.04	0.04	0.04	30.60	-2.55
ME	0.01	0.01	0.01	0.01		
VR5 RMSE	0.06	0.07	0.07	0.08	31.20	-3.22
ME	0.05	0.05	0.06	0.06		
VR6 RMSE	0.05	0.05	0.05	0.04	29.60	-2.56
ME	-0.03	-0.03	-0.02	-0.02		
SS2 RMSE	0.13	0.12	0.09	0.08	25.40	-1.90
ME	-0.06	-0.05	0.03	0.02		
SS4 RMSE	0.11	0.11	0.06	0.07	45.30	-4.03
ME	-0.05	-0.04	-0.02	0.00		
SS5 RMSE	0.09	0.09	0.08	0.09	57.20	-4.50
ME	0.07	0.07	0.07	0.08		
SS6 RMSE	0.07	0.07	0.07	0.08	66.30	-5.41
ME	0.04	0.04	0.05	0.06		
SS8 RMSE	0.08	0.09	0.07	0.08	64.70	-5.08
ME	-0.04	-0.04	-0.02	-0.02		
SS9 RMSE	0.04	0.04	0.04	0.04	58.50	-4.39
ME	0.00	0.00	0.01	0.01		
CP3 RMSE	0.16	0.16	0.10	0.10	38.40	-3.38
ME	-0.13	-0.13	-0.08	-0.07		
KB1 RMSE	0.30	0.29	0.21	0.20	48.00	-3.85
ME	-0.26	-0.25	-0.18	-0.17		
total RMSE	0.12	0.12	0.09	0.09		
ME	-0.03	-0.03	-0.00	0.00		

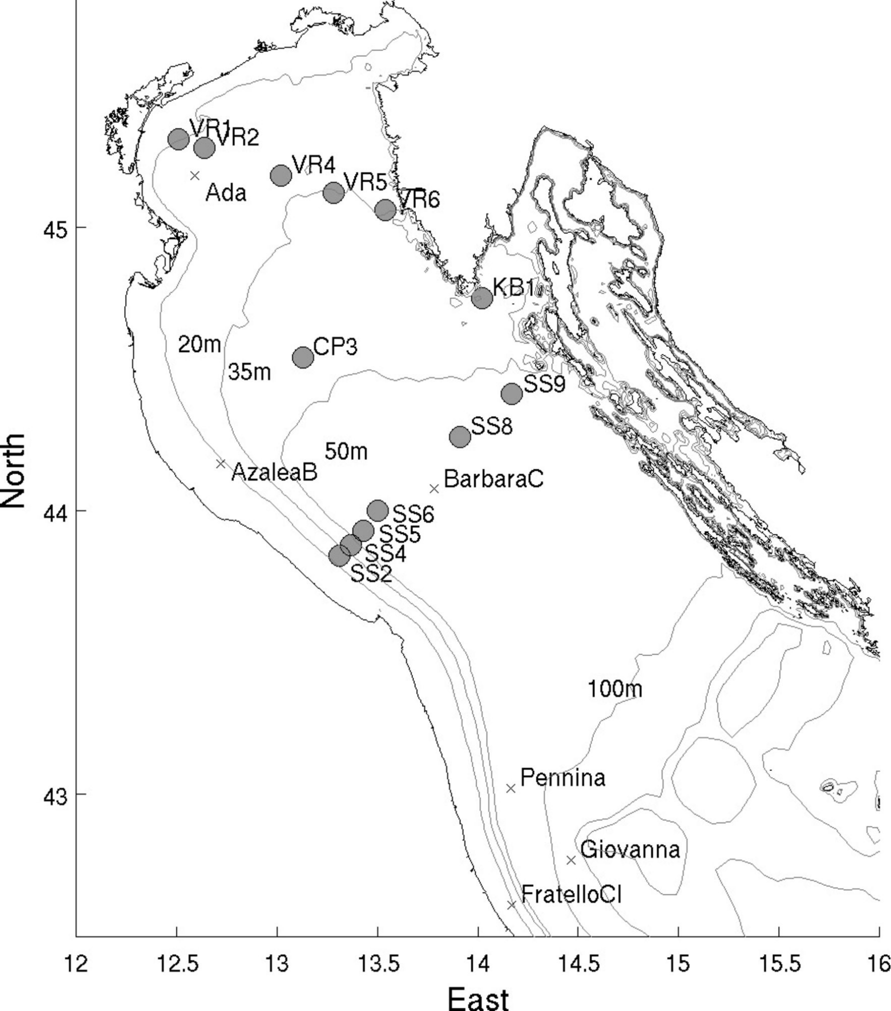

VR1
VR2
VR4
VR5
VR6
Ada
KB1
20m
35m
CP3
SS9
SS8
50m
AzaleaB
BarbaraC
SS6
SS5
SS4
SS2
100m
Pennina
Giovanna
FratelloCl
45
44
43
North
12
12.5
13
13.5
14
14.5
15
15.5
16
East

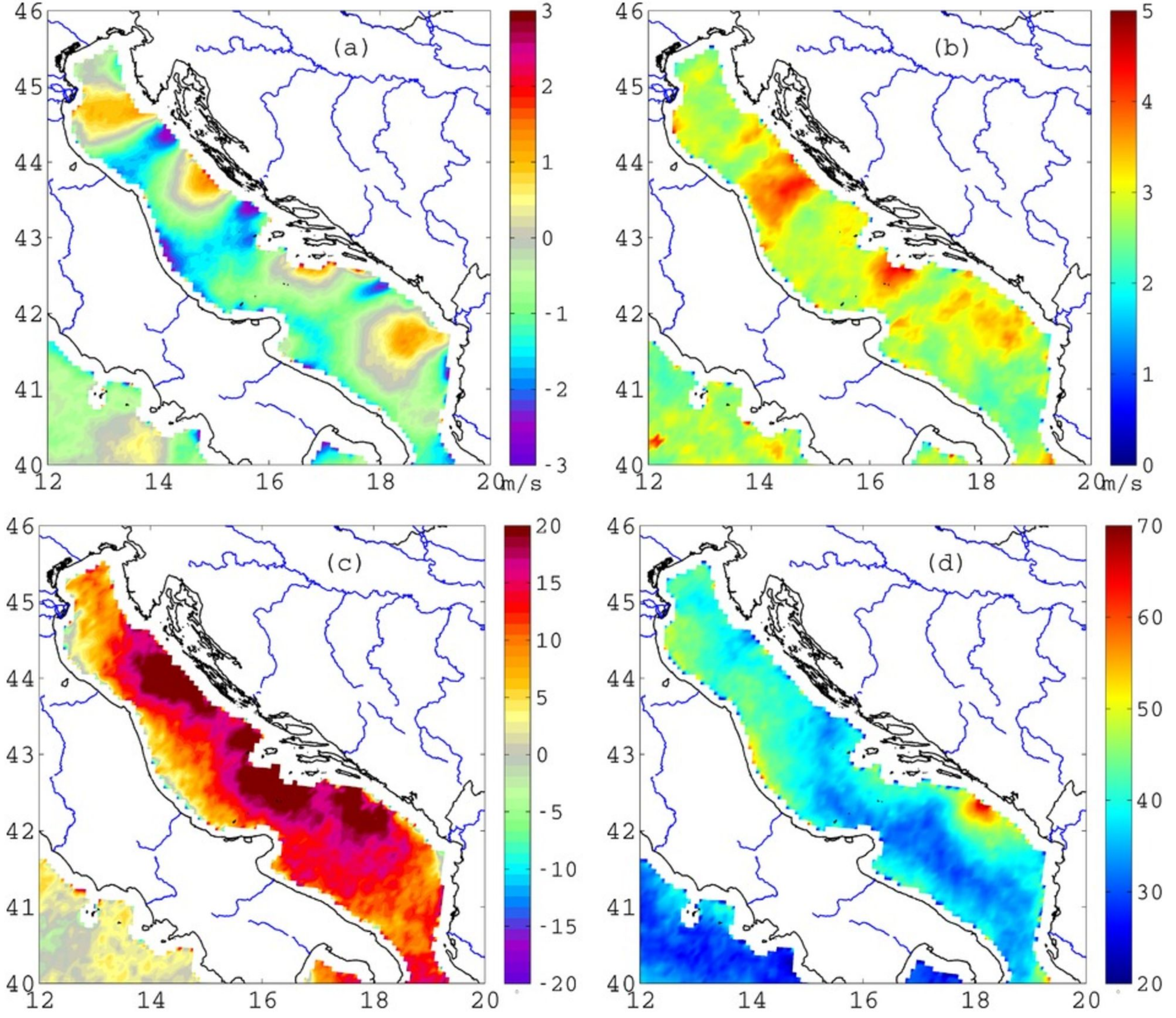

(a)
(b)
(c)
(d)
m/s
m/s
46
45
44
43
42
41
40
12
14
16
18
20
3
2
1
0
-1
-2
-3
5
4
3
2
1
0
20
15
10
5
0
-5
-10
-15
-20
70
60
50
40
30
20

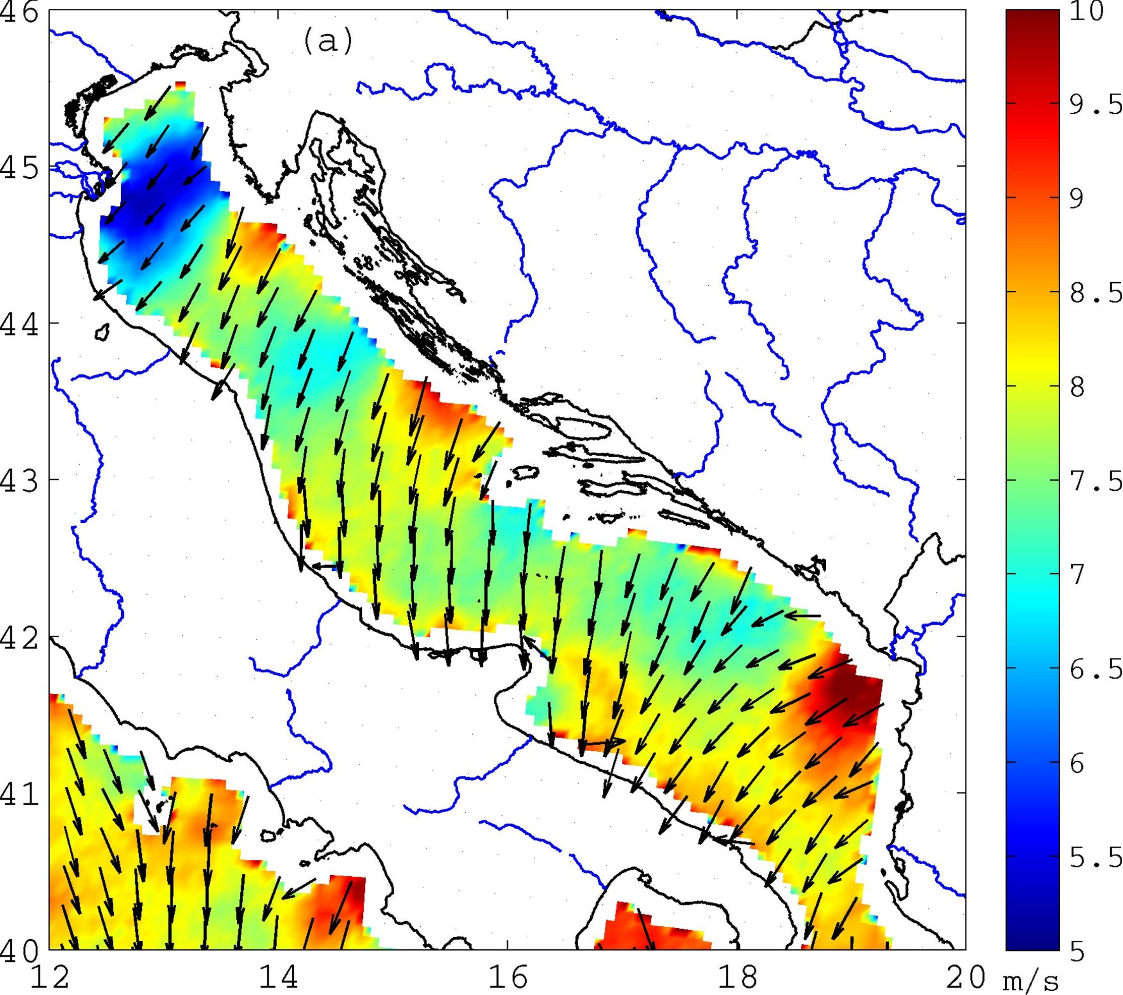
(a)
46
45
44
43
42
41
40
12
14
16
18
20
10
9.5
9
8.5
8
7.5
7
6.5
6
5.5
5
m/s

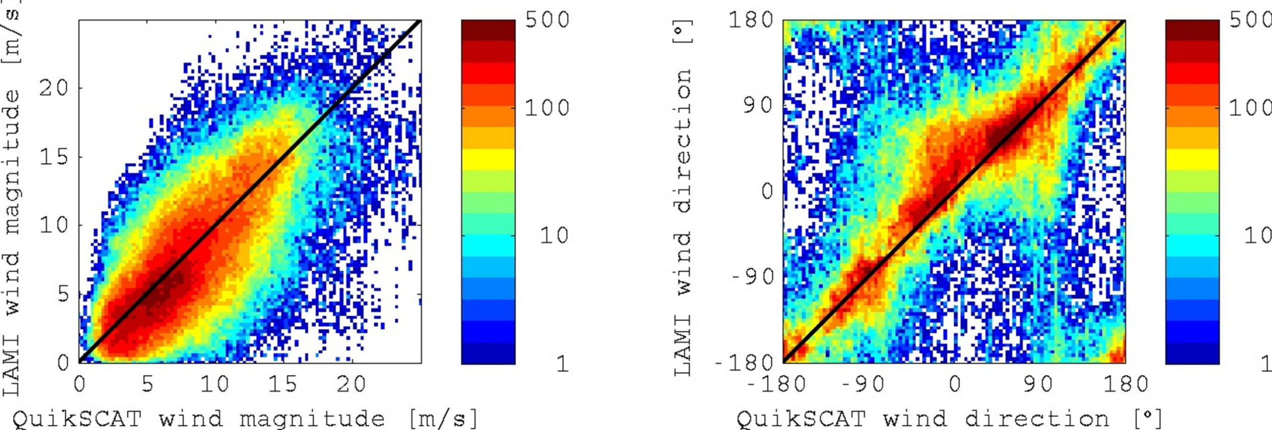
LAMI wind magnitude [m/s]
QuikSCAT wind magnitude [m/s]
0
5
10
15
20
500
100
10
1
LAMI wind direction [°]
QuikSCAT wind direction [°]
-180
-90
0
90
180
500
100
10
1

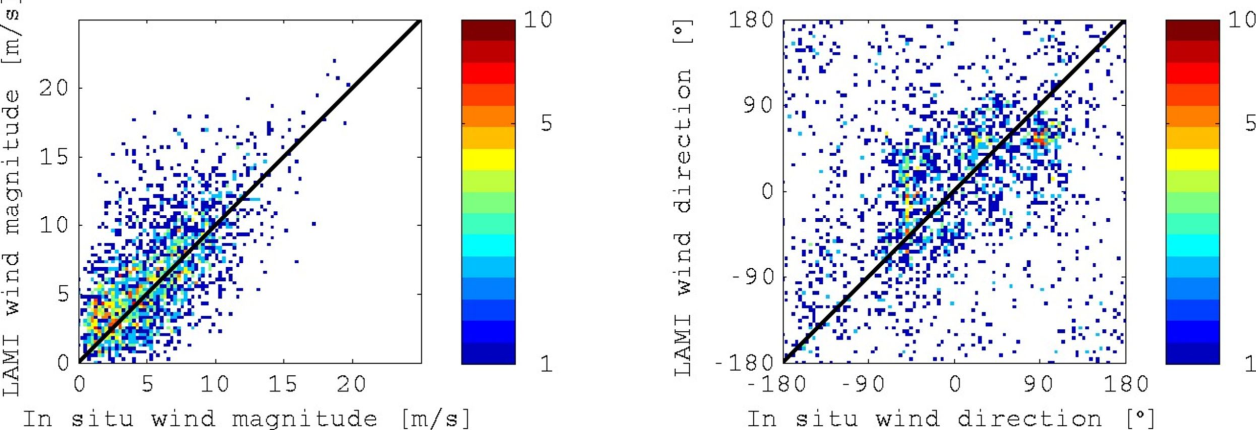

LAMI wind magnitude [m/s]
In situ wind magnitude [m/s]
0
5
10
15
20
10
5
1
LAMI wind direction [°]
In situ wind direction [°]
-180
-90
0
90
180
10
5
1

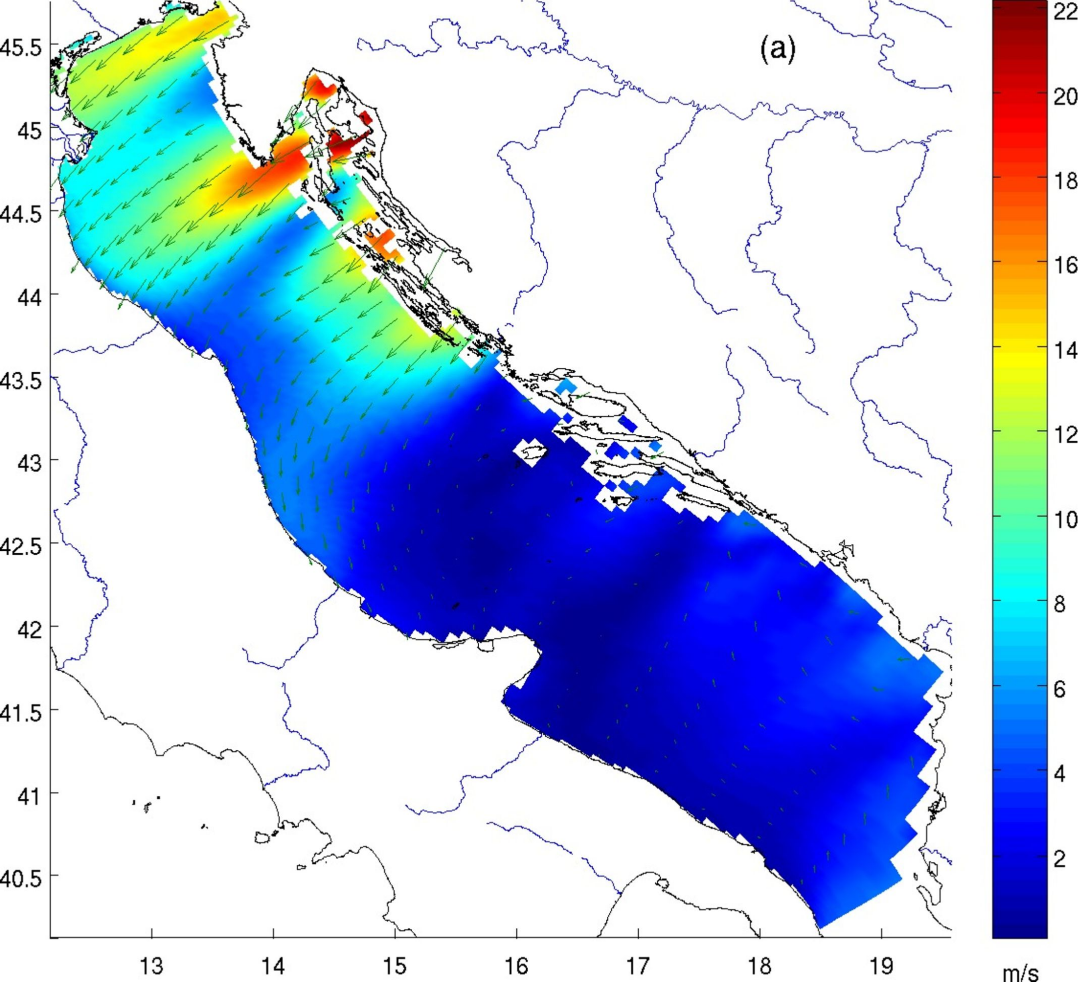
(a)
45.5
45
44.5
44
43.5
43
42.5
42
41.5
41
40.5
13
14
15
16
17
18
19
22
20
18
16
14
12
10
8
6
4
2
m/s

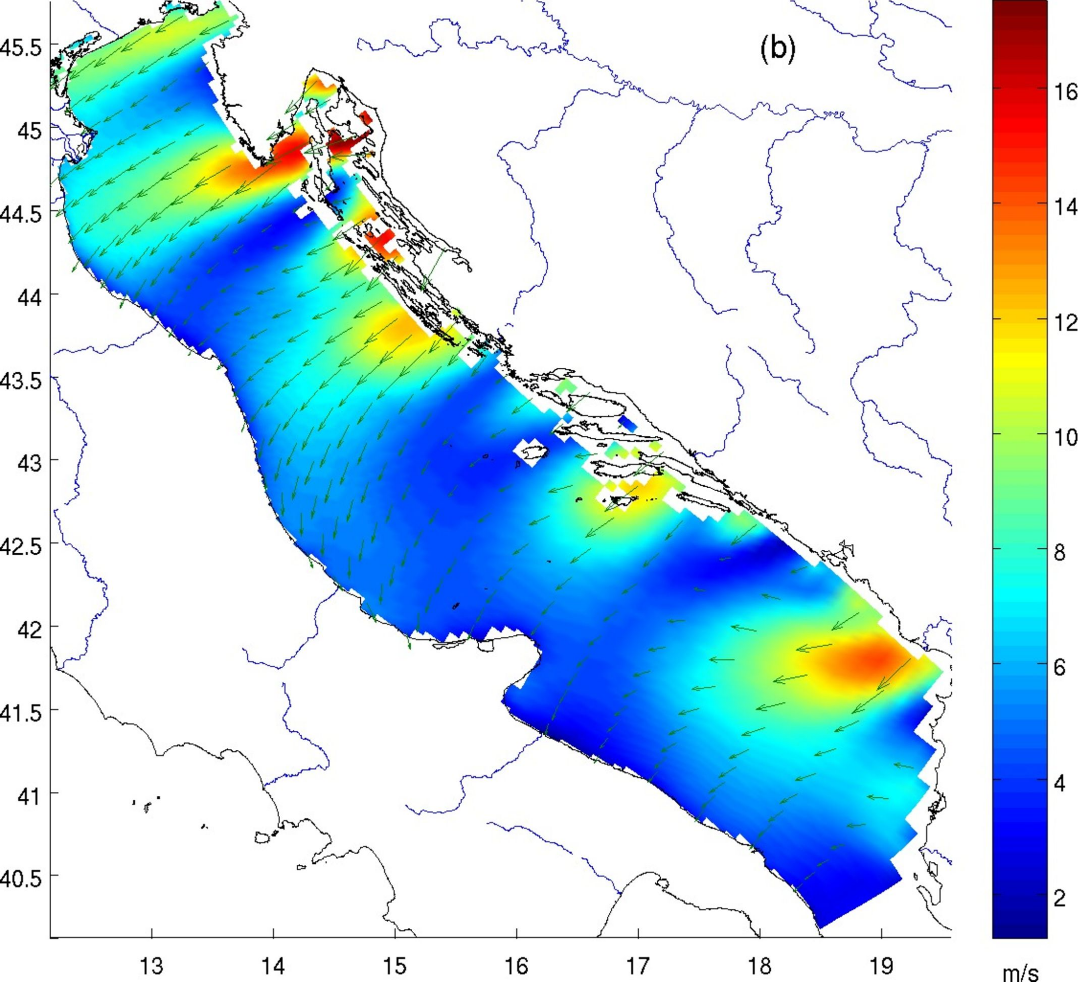

(b)
45.5
45
44.5
44
43.5
43
42.5
42
41.5
41
40.5
13
14
15
16
17
18
19
16
14
12
10
8
6
4
2
m/s

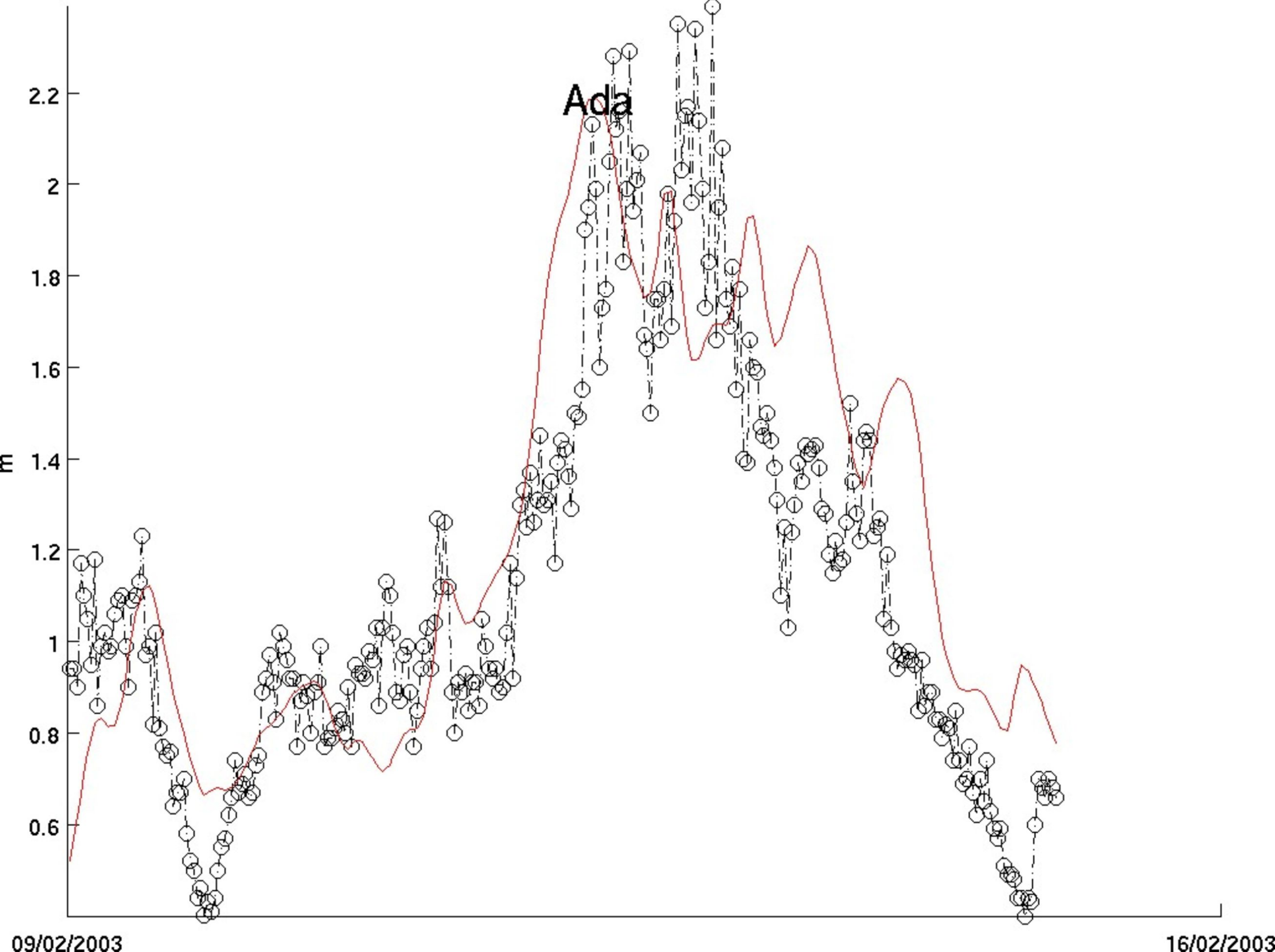
Ada
m
2.2
2
1.8
1.6
1.4
1.2
1
0.8
0.6
09/02/2003
16/02/2003

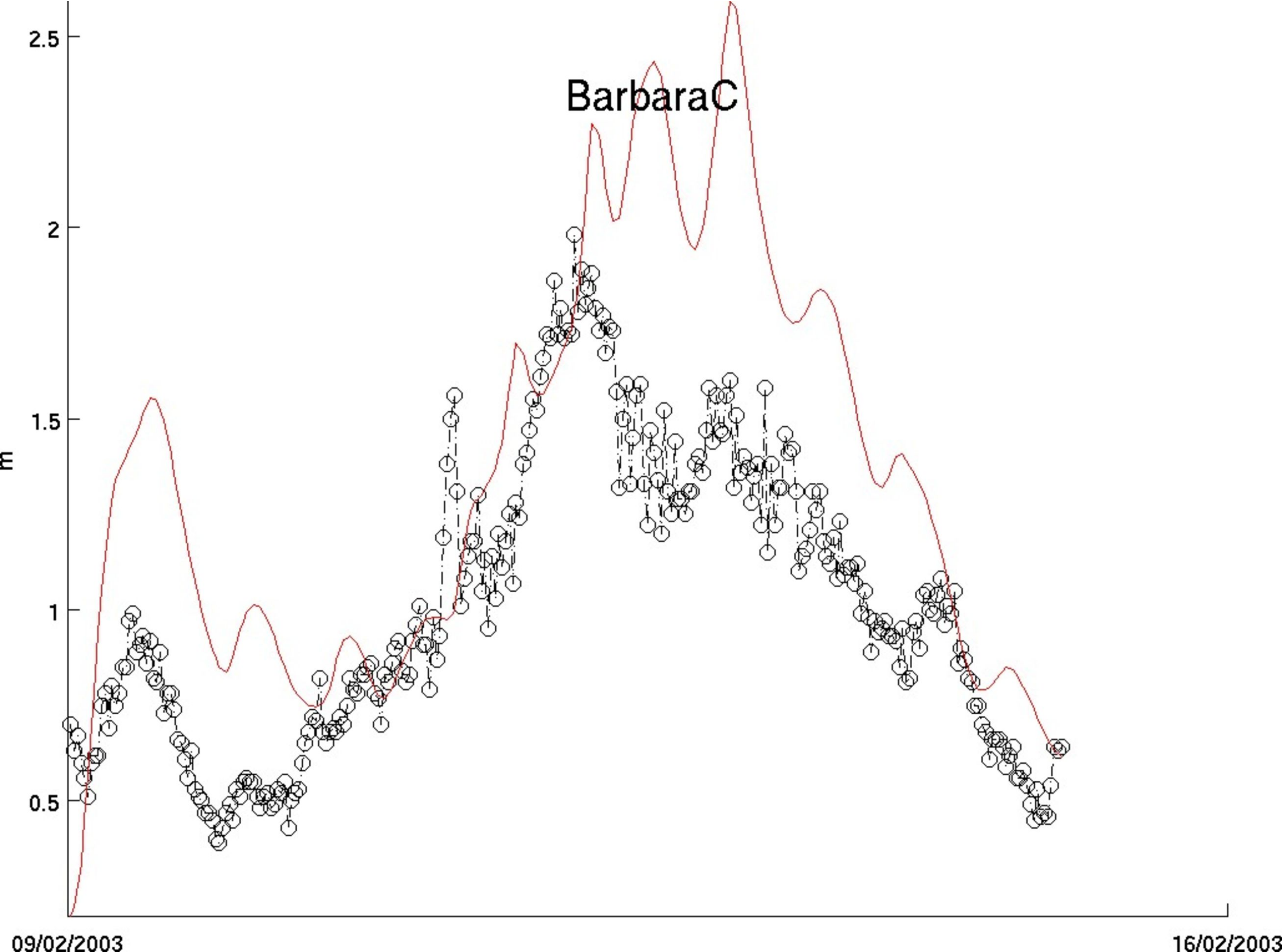
BarbaraC
2.5
2
1.5
1
0.5
m
09/02/2003
16/02/2003

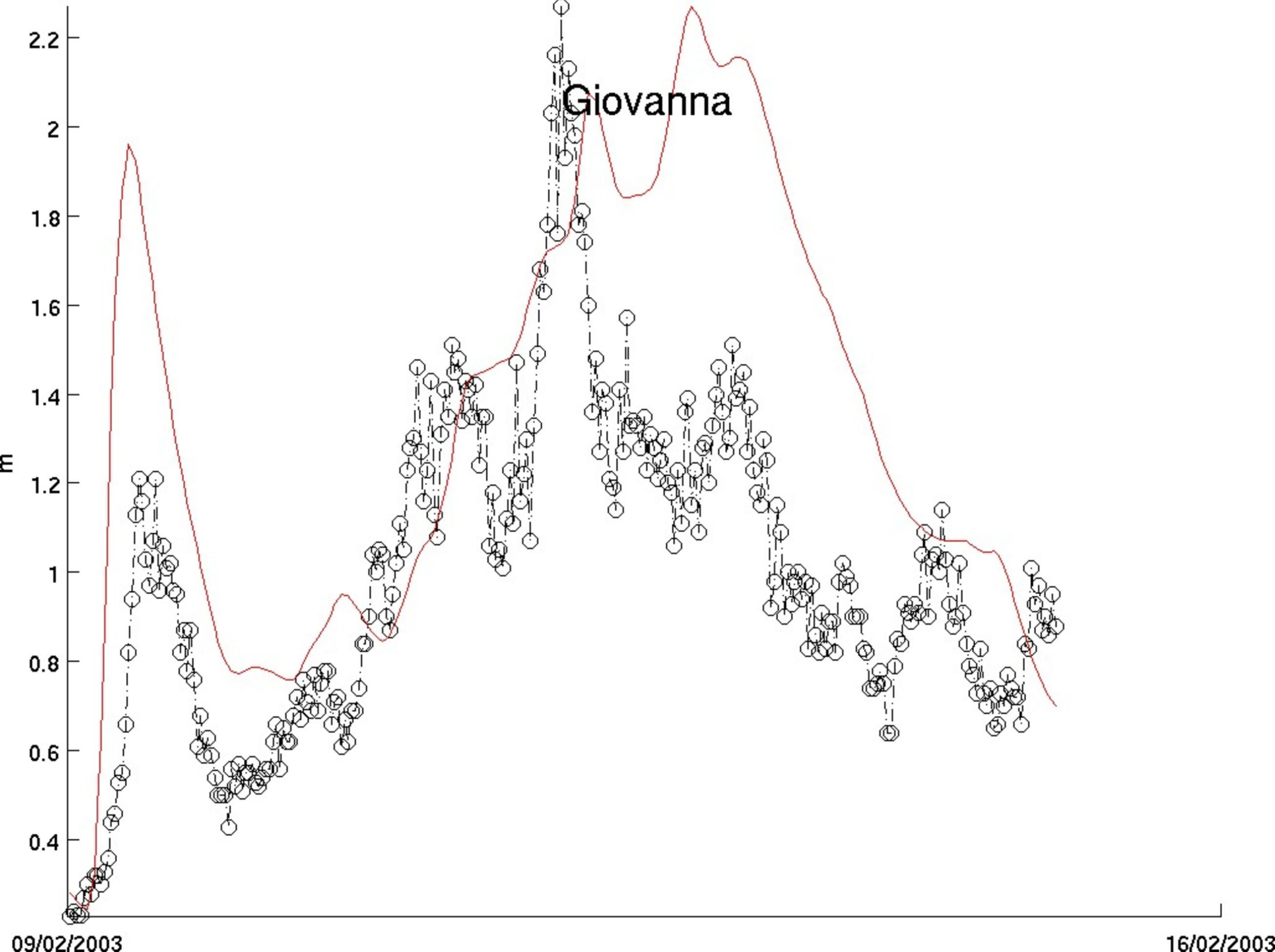

Giovanna
m
2.2
2
1.8
1.6
1.4
1.2
1
0.8
0.6
0.4
09/02/2003
16/02/2003

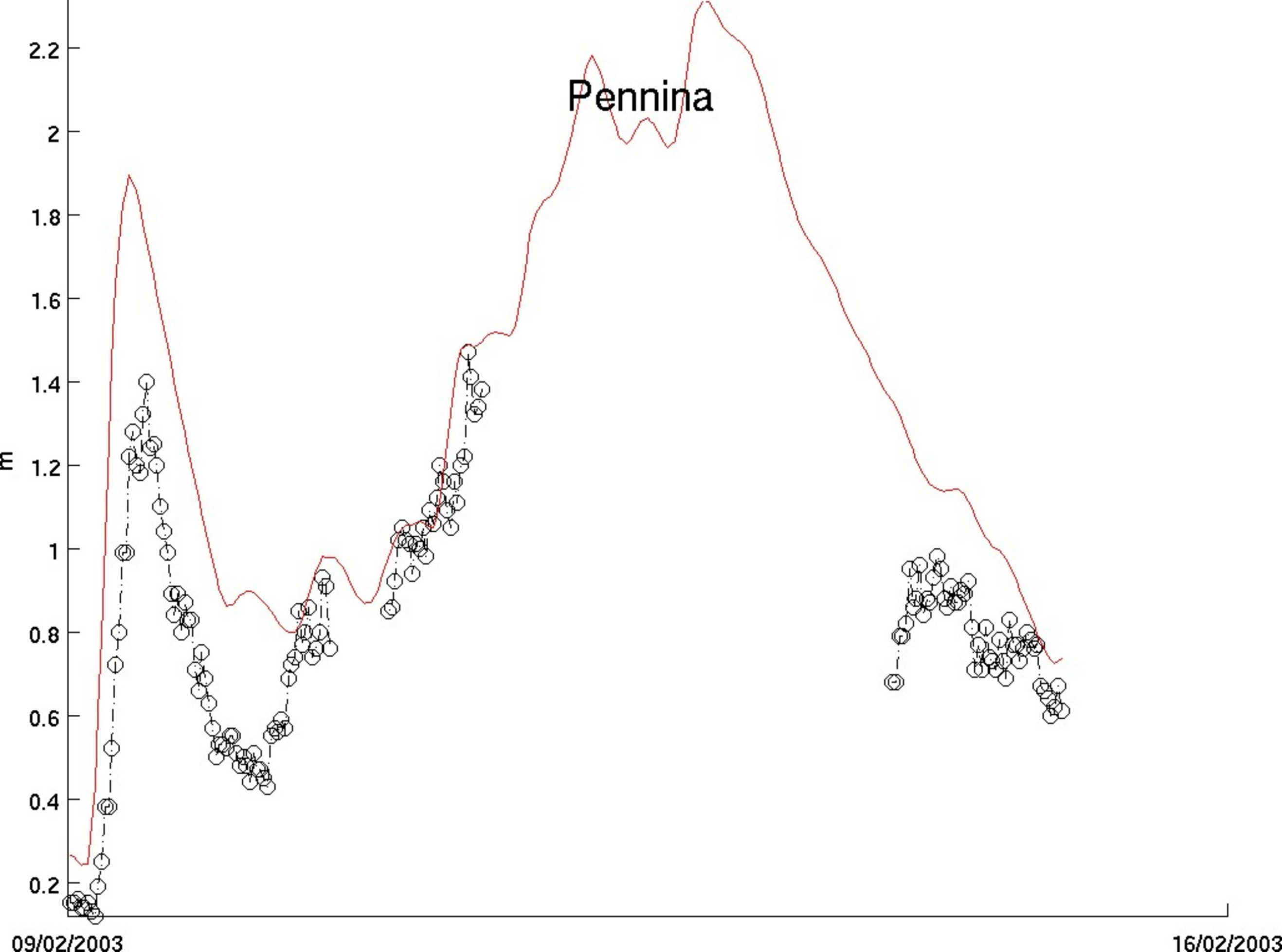

Pennina
m
2.2
2
1.8
1.6
1.4
1.2
1
0.8
0.6
0.4
0.2
09/02/2003
16/02/2003

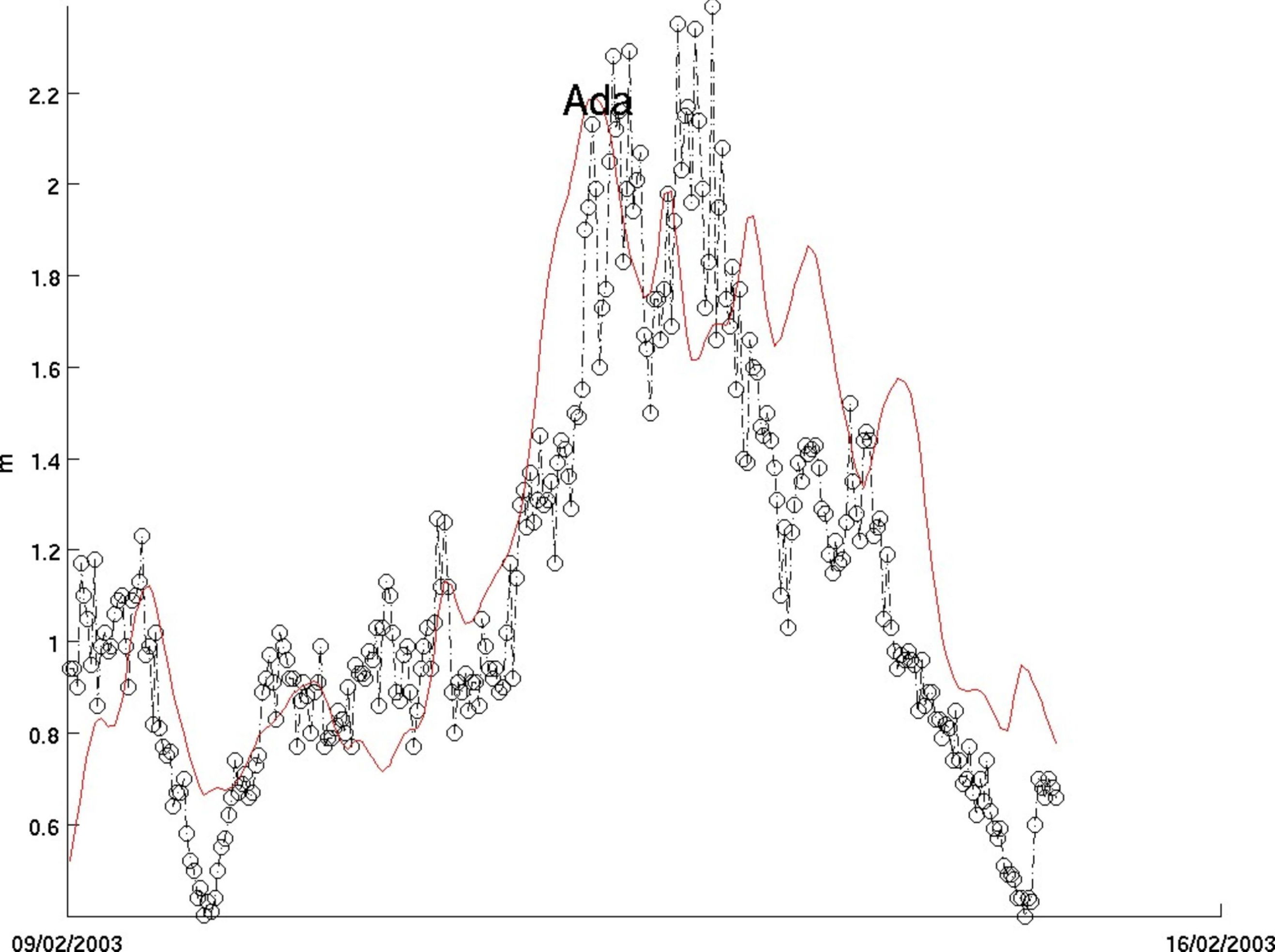

Ada
m
2.2
2
1.8
1.6
1.4
1.2
1
0.8
0.6
09/02/2003
16/02/2003

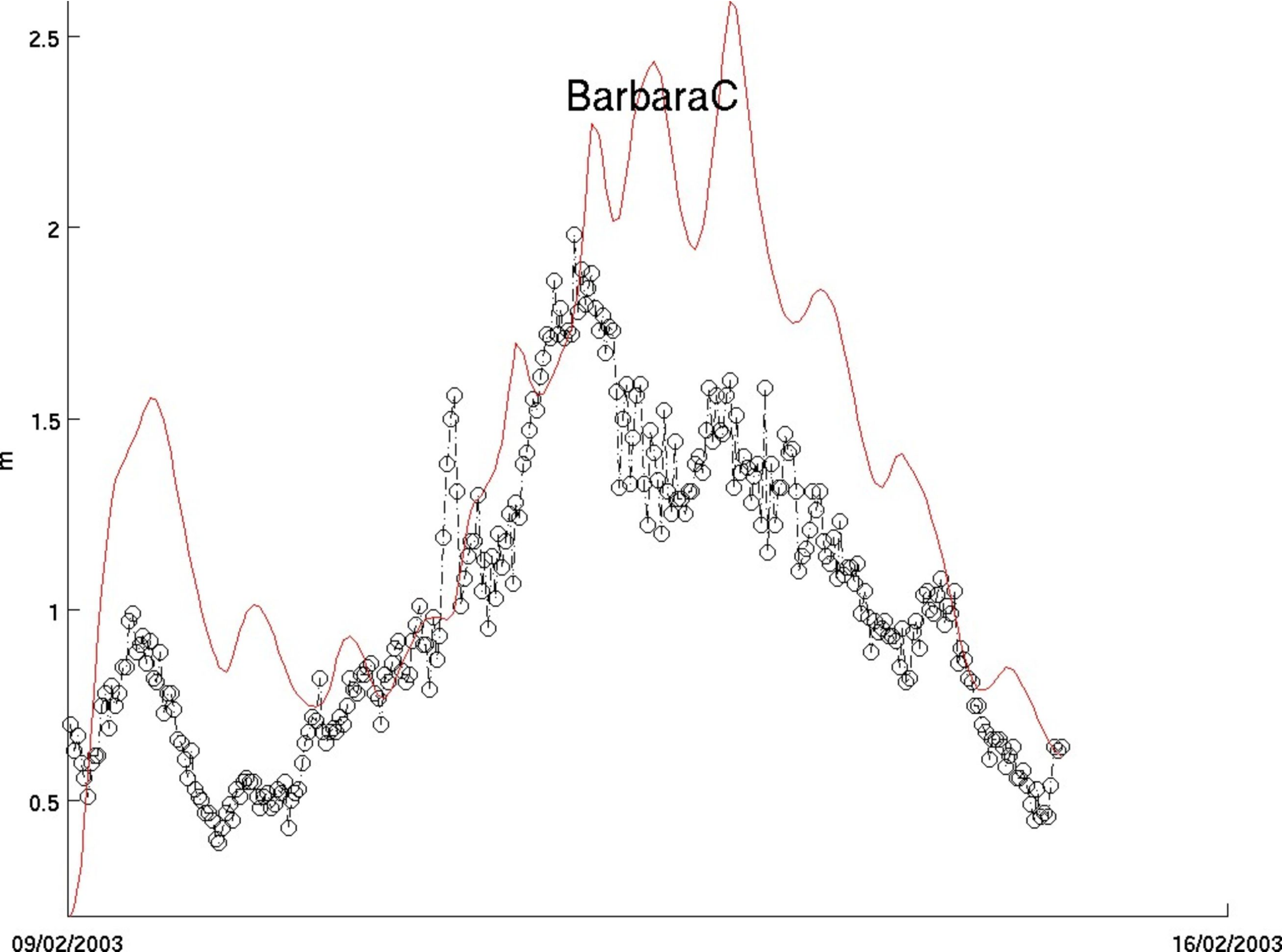

BarbaraC
2.5
2
1.5
1
0.5
m
09/02/2003
16/02/2003

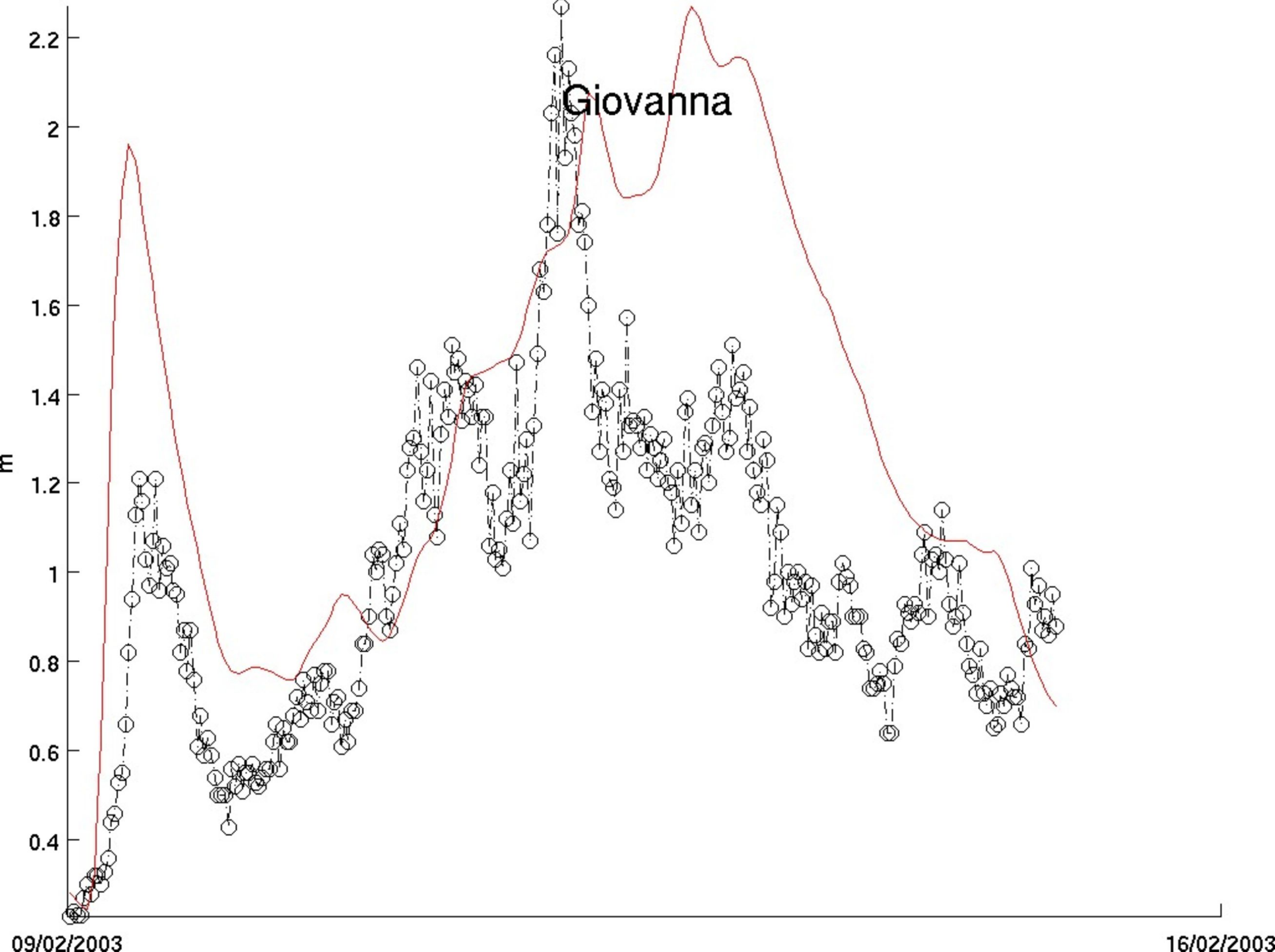

Giovanna
m
2.2
2
1.8
1.6
1.4
1.2
1
0.8
0.6
0.4
09/02/2003
16/02/2003

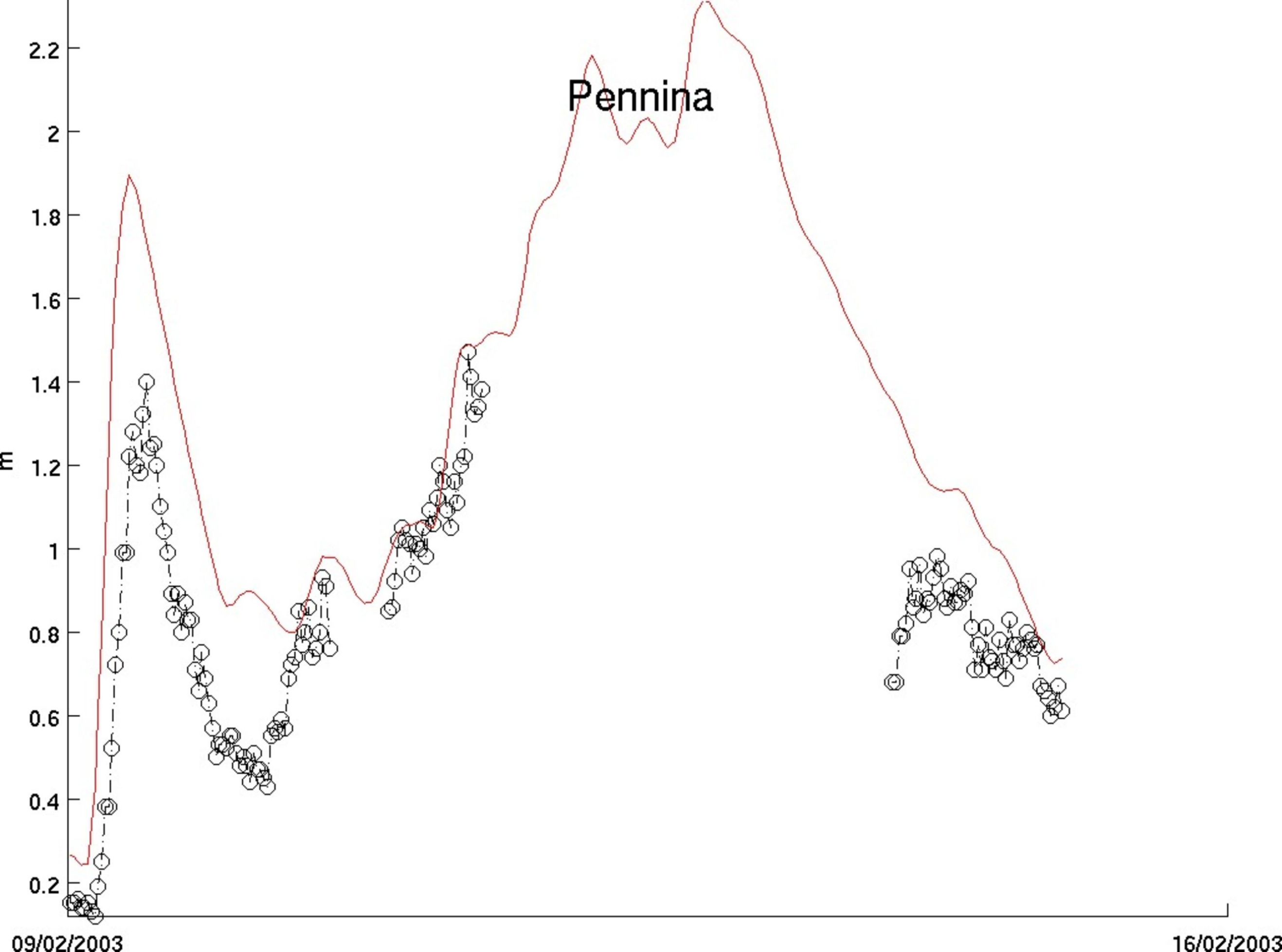

Pennina
m
2.2
2
1.8
1.6
1.4
1.2
1
0.8
0.6
0.4
0.2
09/02/2003
16/02/2003

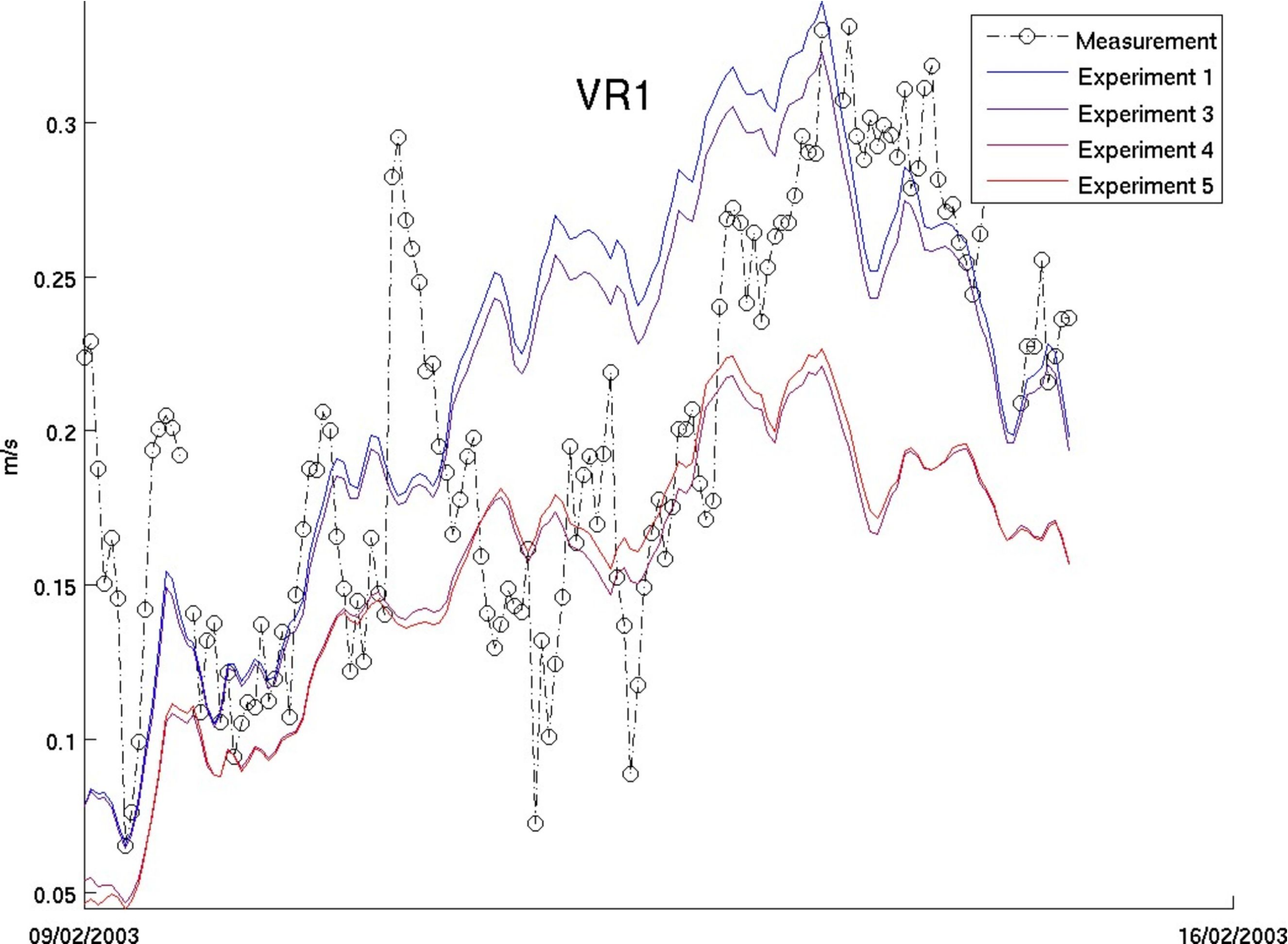
VR1
Measurement
Experiment 1
Experiment 3
Experiment 4
Experiment 5
m/s
0.3
0.25
0.2
0.15
0.1
0.05
09/02/2003
16/02/2003

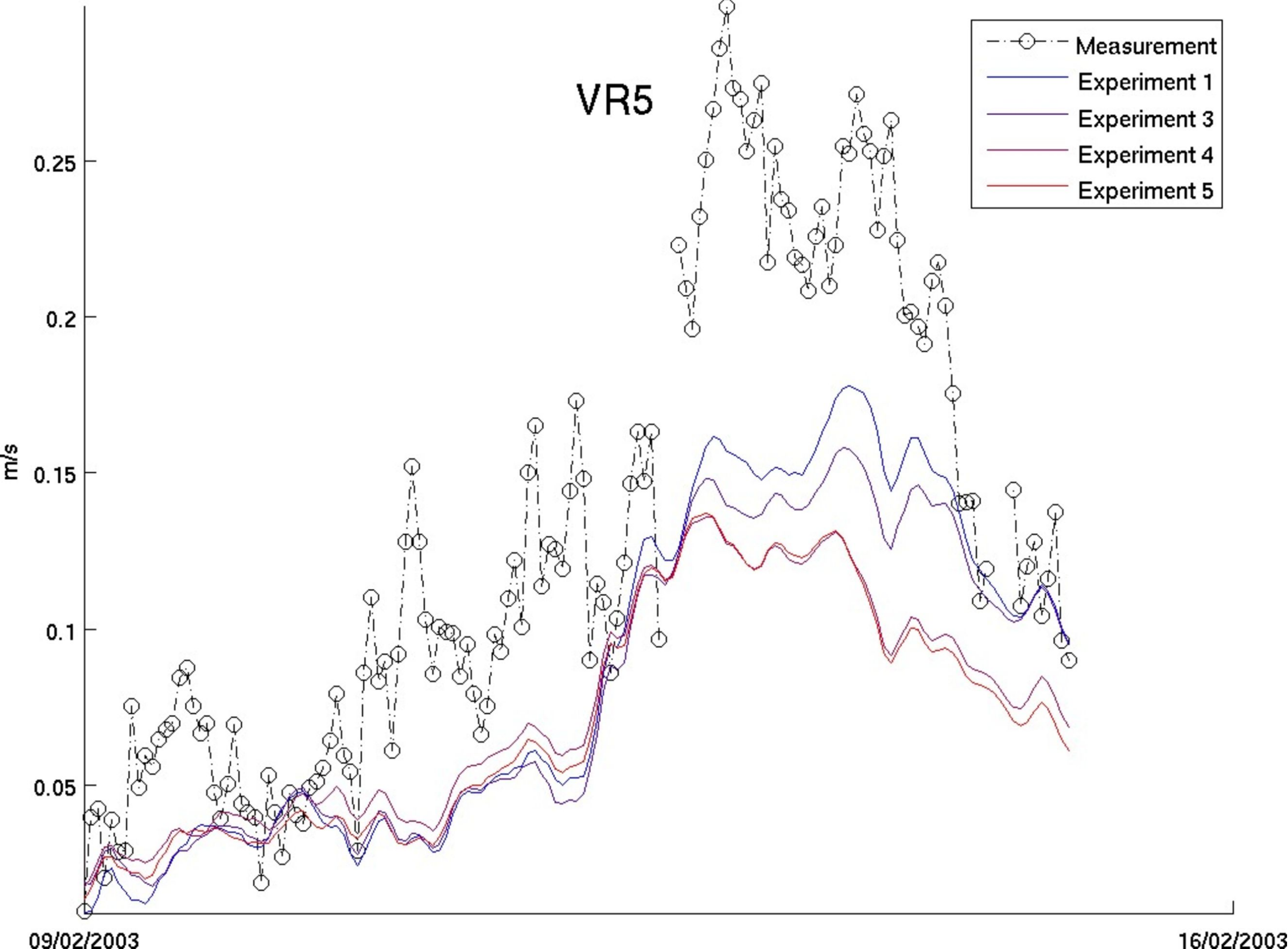
VR5
Measurement
Experiment 1
Experiment 3
Experiment 4
Experiment 5
m/s
0.25
0.2
0.15
0.1
0.05
09/02/2003
16/02/2003

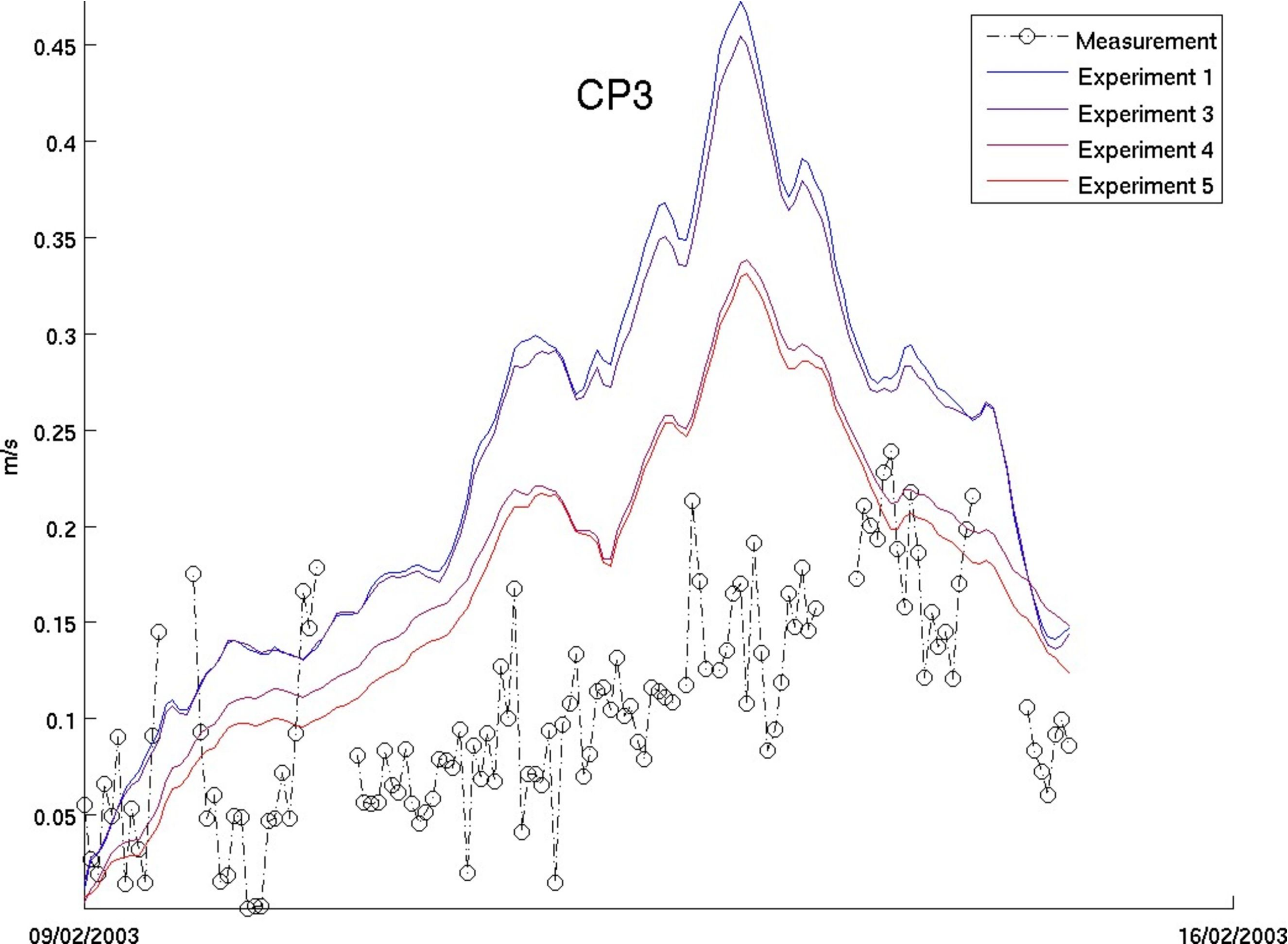

CP3
Measurement
Experiment 1
Experiment 3
Experiment 4
Experiment 5
m/s
0.45
0.4
0.35
0.3
0.25
0.2
0.15
0.1
0.05
09/02/2003
16/02/2003

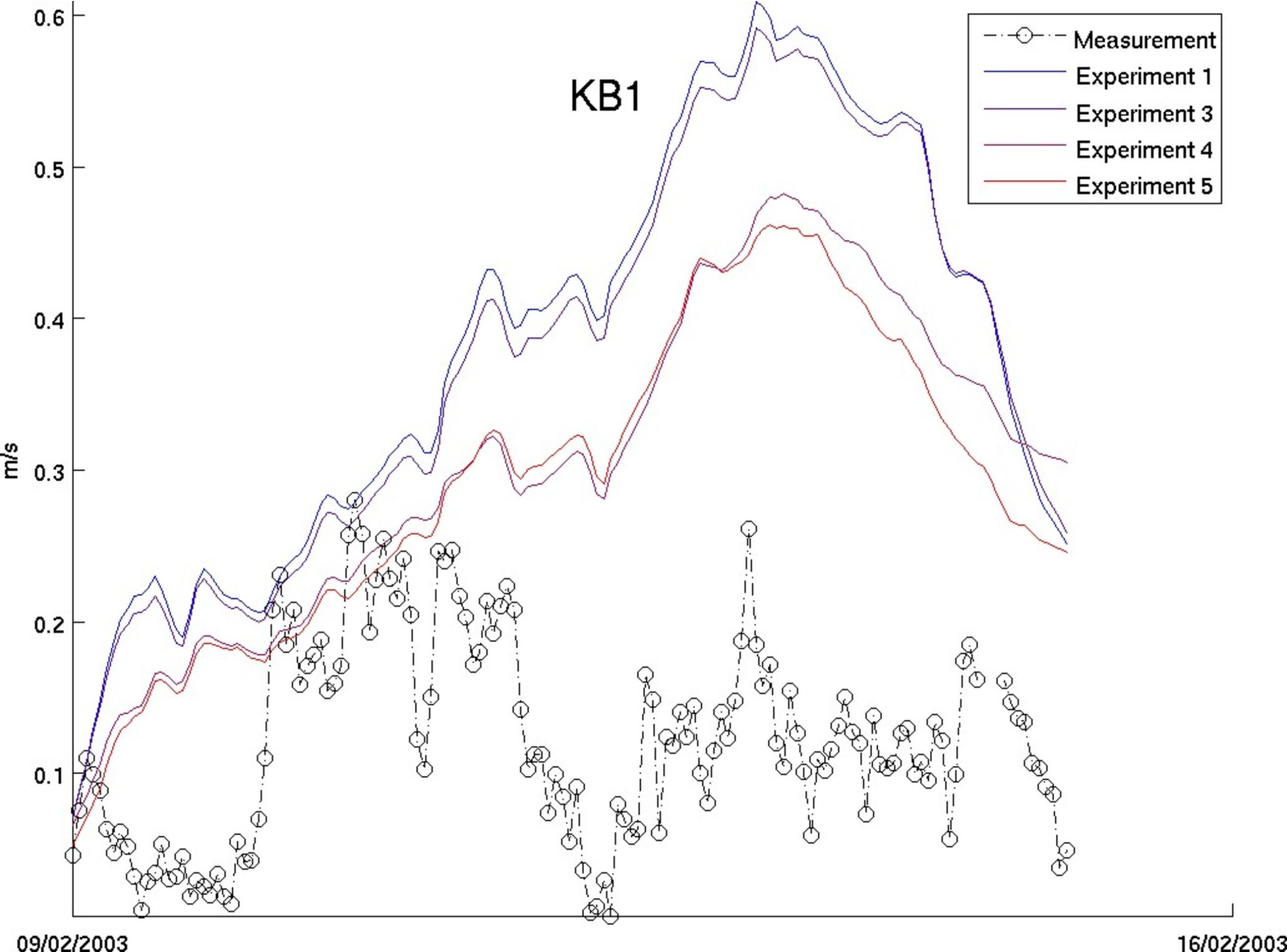

KB1
Measurement
Experiment 1
Experiment 3
Experiment 4
Experiment 5
m/s
0.6
0.5
0.4
0.3
0.2
0.1
09/02/2003
16/02/2003

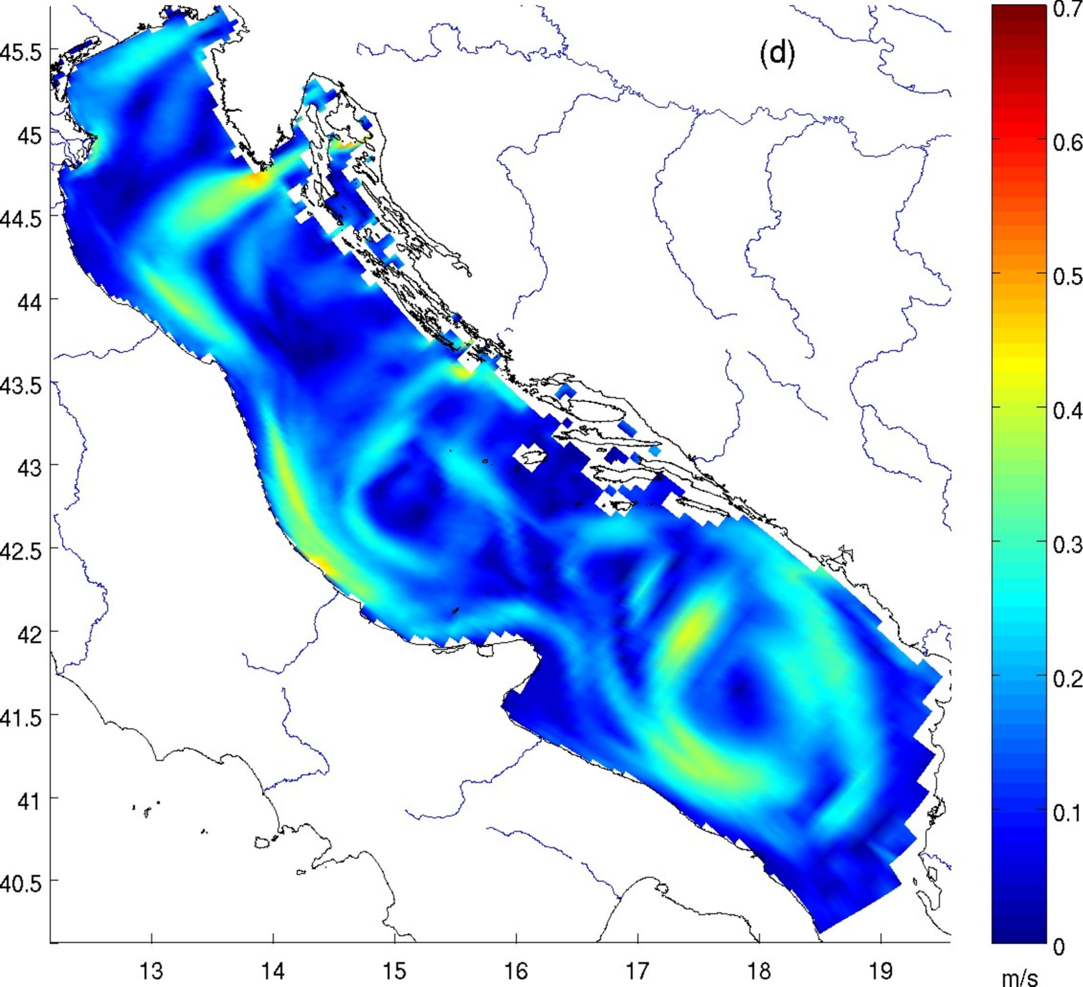

(d)
45.5
45
44.5
44
43.5
43
42.5
42
41.5
41
40.5
13
14
15
16
17
18
19
0.7
0.6
0.5
0.4
0.3
0.2
0.1
0
m/s

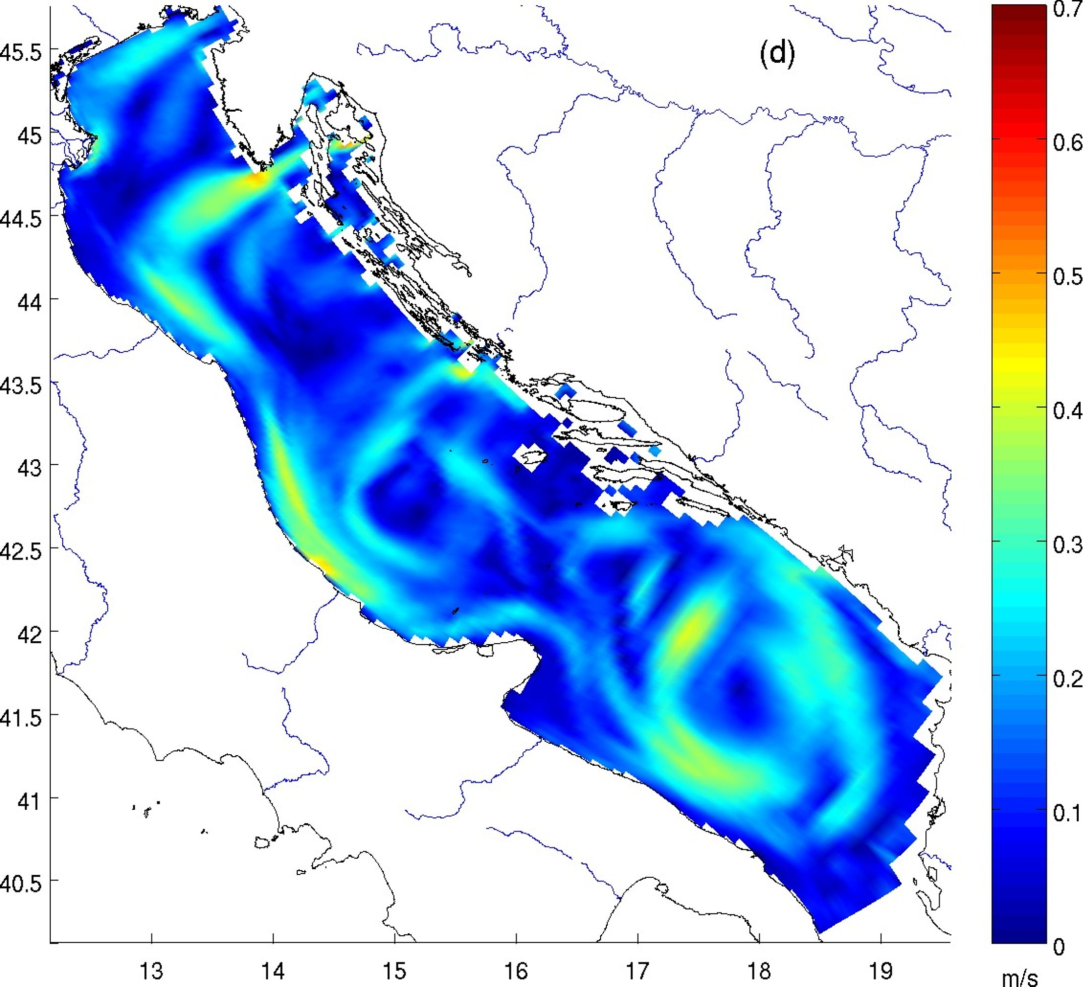
(d)
45.5
45
44.5
44
43.5
43
42.5
42
41.5
41
40.5
13
14
15
16
17
18
19
0.7
0.6
0.5
0.4
0.3
0.2
0.1
0
m/s

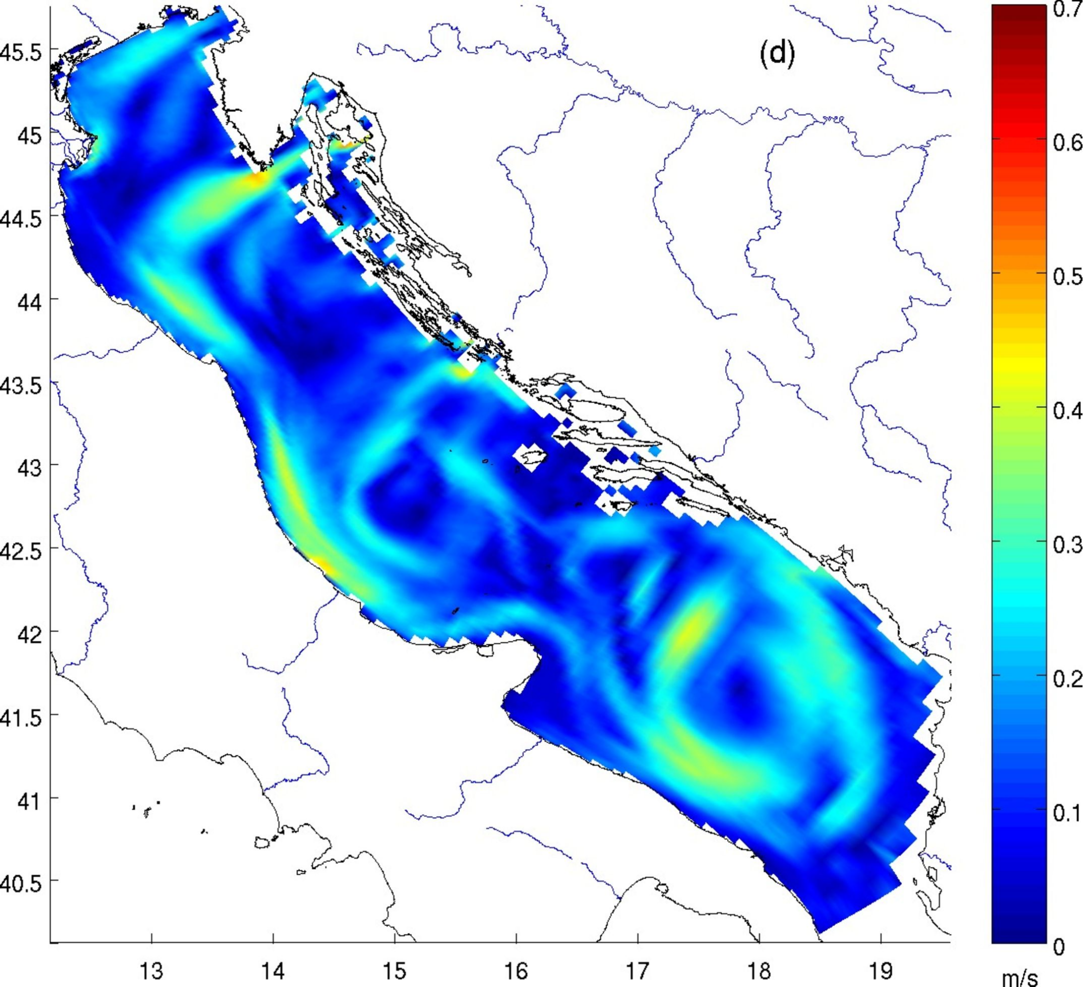
(d)
45.5
45
44.5
44
43.5
43
42.5
42
41.5
41
40.5
13
14
15
16
17
18
19
0.7
0.6
0.5
0.4
0.3
0.2
0.1
0
m/s

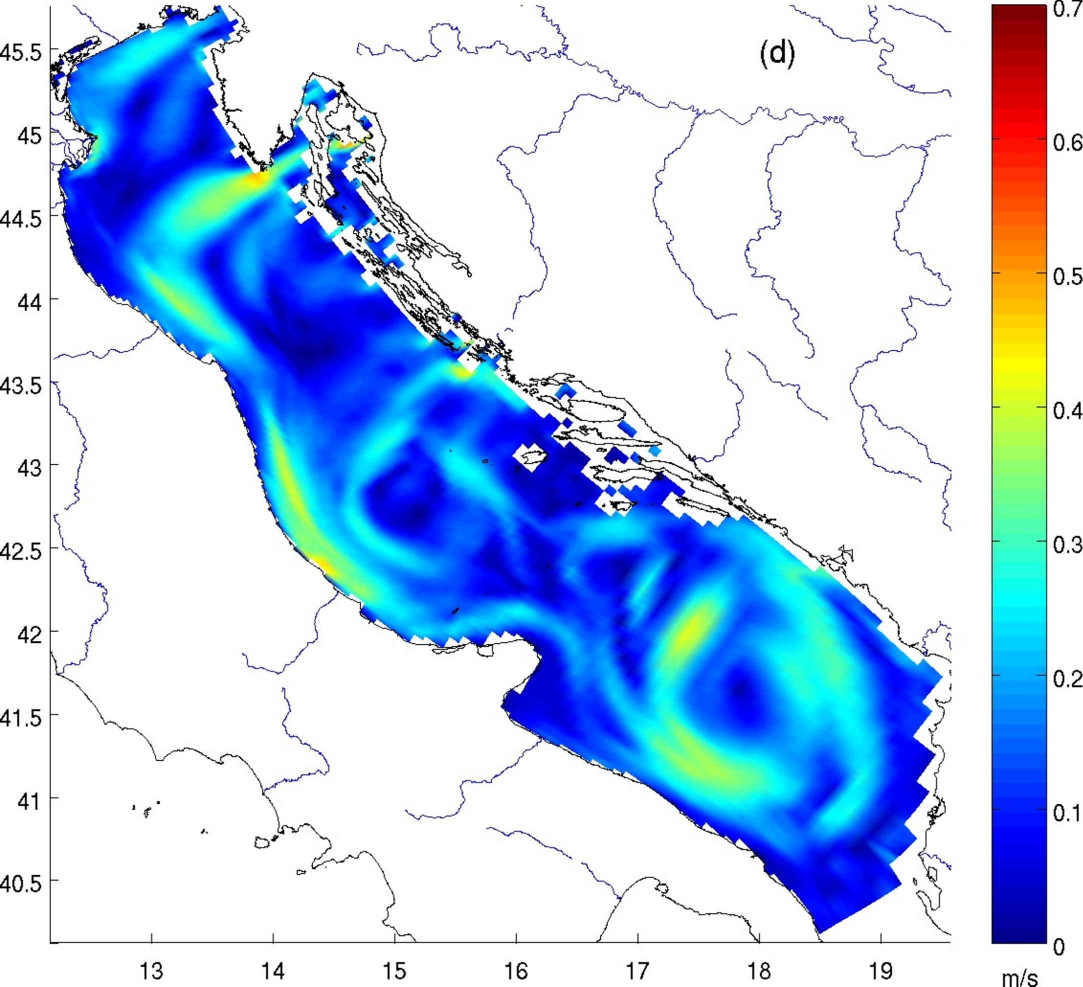
(d)
45.5
45
44.5
44
43.5
43
42.5
42
41.5
41
40.5
13
14
15
16
17
18
19
0.7
0.6
0.5
0.4
0.3
0.2
0.1
0
m/s

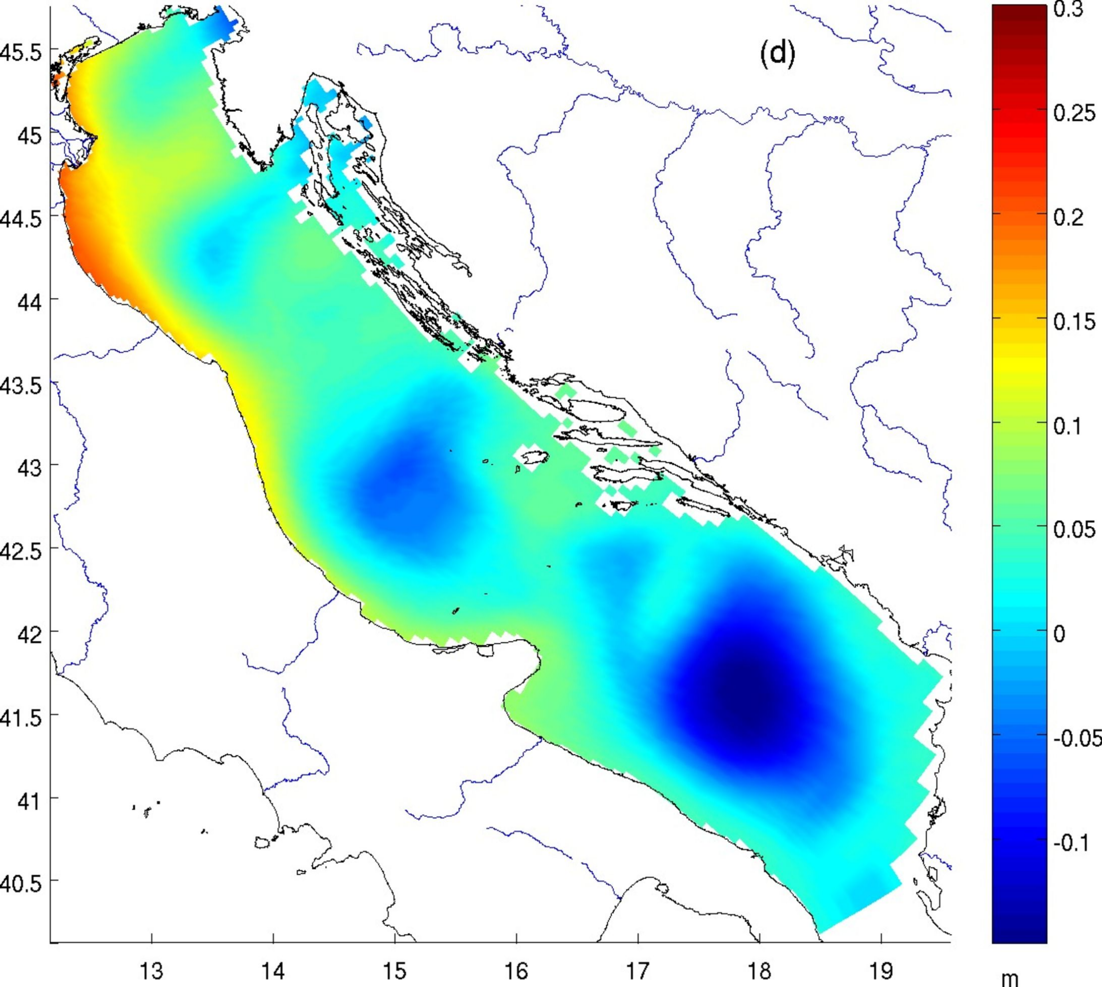

(d)
45.5
45
44.5
44
43.5
43
42.5
42
41.5
41
40.5
13
14
15
16
17
18
19
0.3
0.25
0.2
0.15
0.1
0.05
0
-0.05
-0.1
m

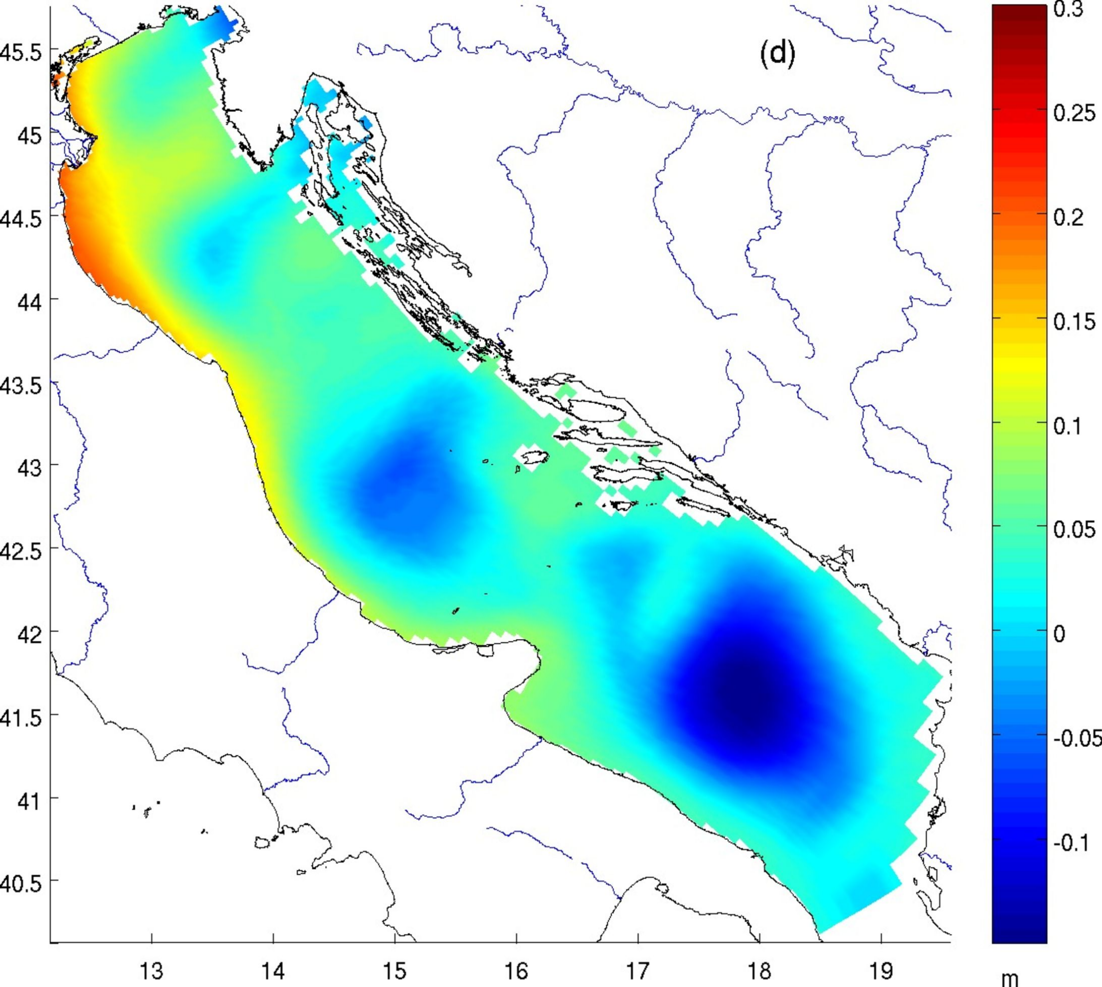

(d)
45.5
45
44.5
44
43.5
43
42.5
42
41.5
41
40.5
13
14
15
16
17
18
19
0.3
0.25
0.2
0.15
0.1
0.05
0
-0.05
-0.1
m

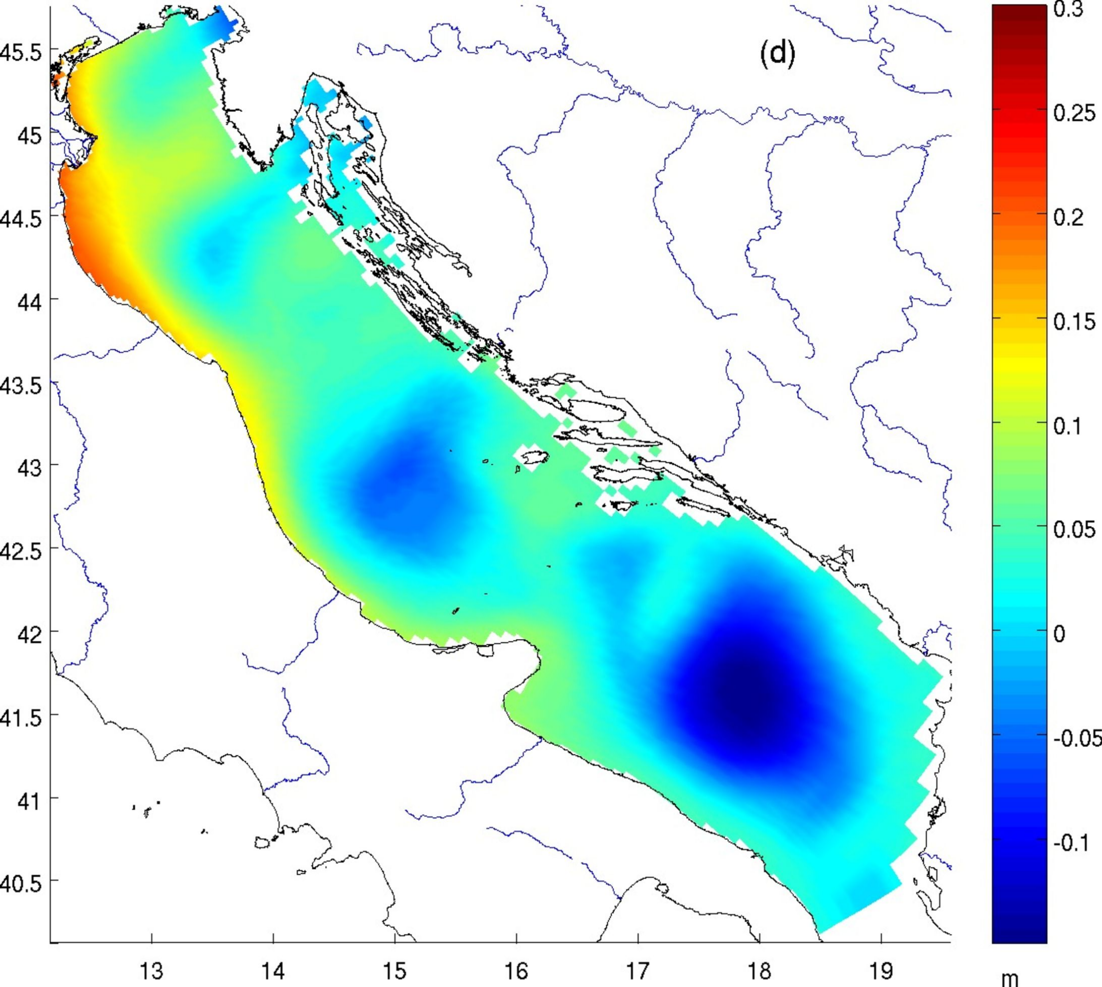

(d)
45.5
45
44.5
44
43.5
43
42.5
42
41.5
41
40.5
13
14
15
16
17
18
19
0.3
0.25
0.2
0.15
0.1
0.05
0
-0.05
-0.1
m

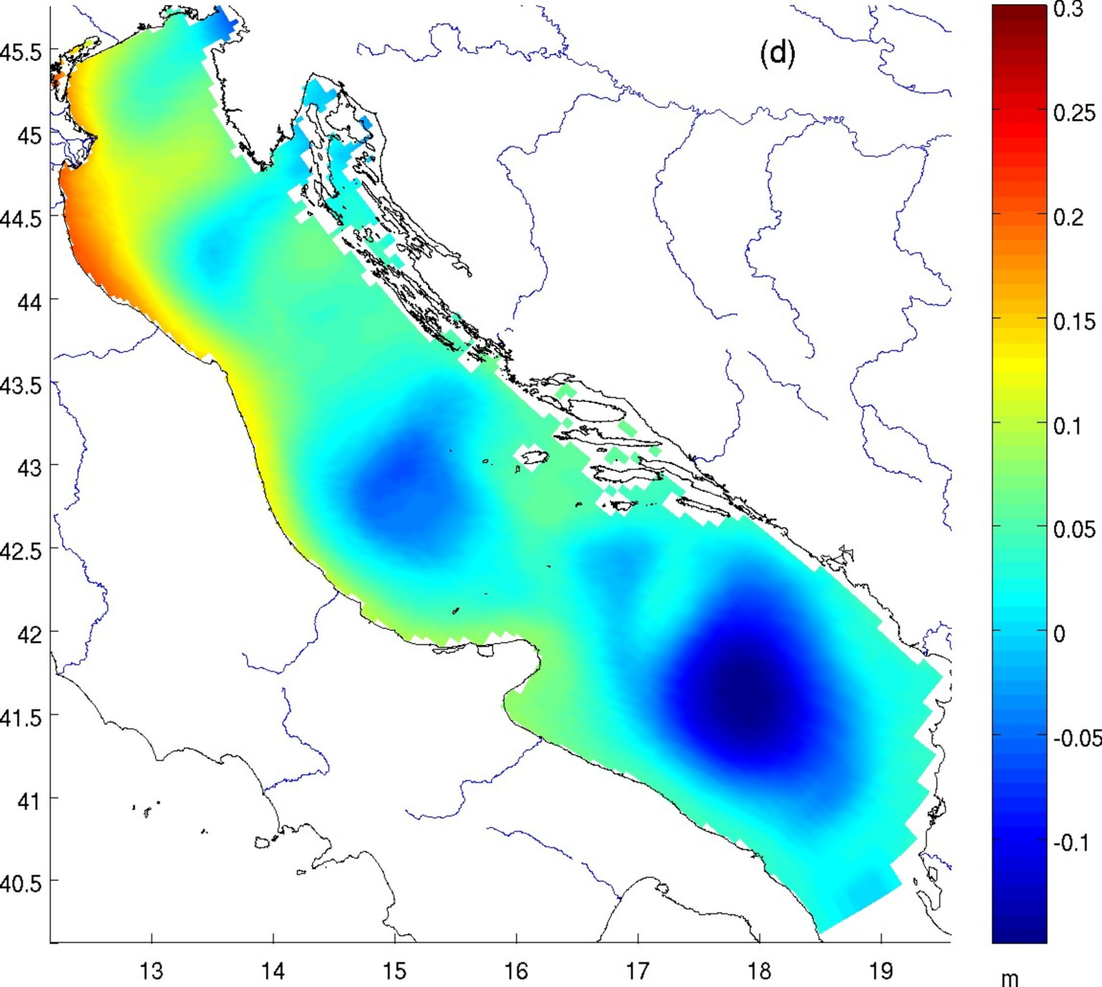
(d)
45.5
45
44.5
44
43.5
43
42.5
42
41.5
41
40.5
13
14
15
16
17
18
19
0.3
0.25
0.2
0.15
0.1
0.05
0
-0.05
-0.1
m

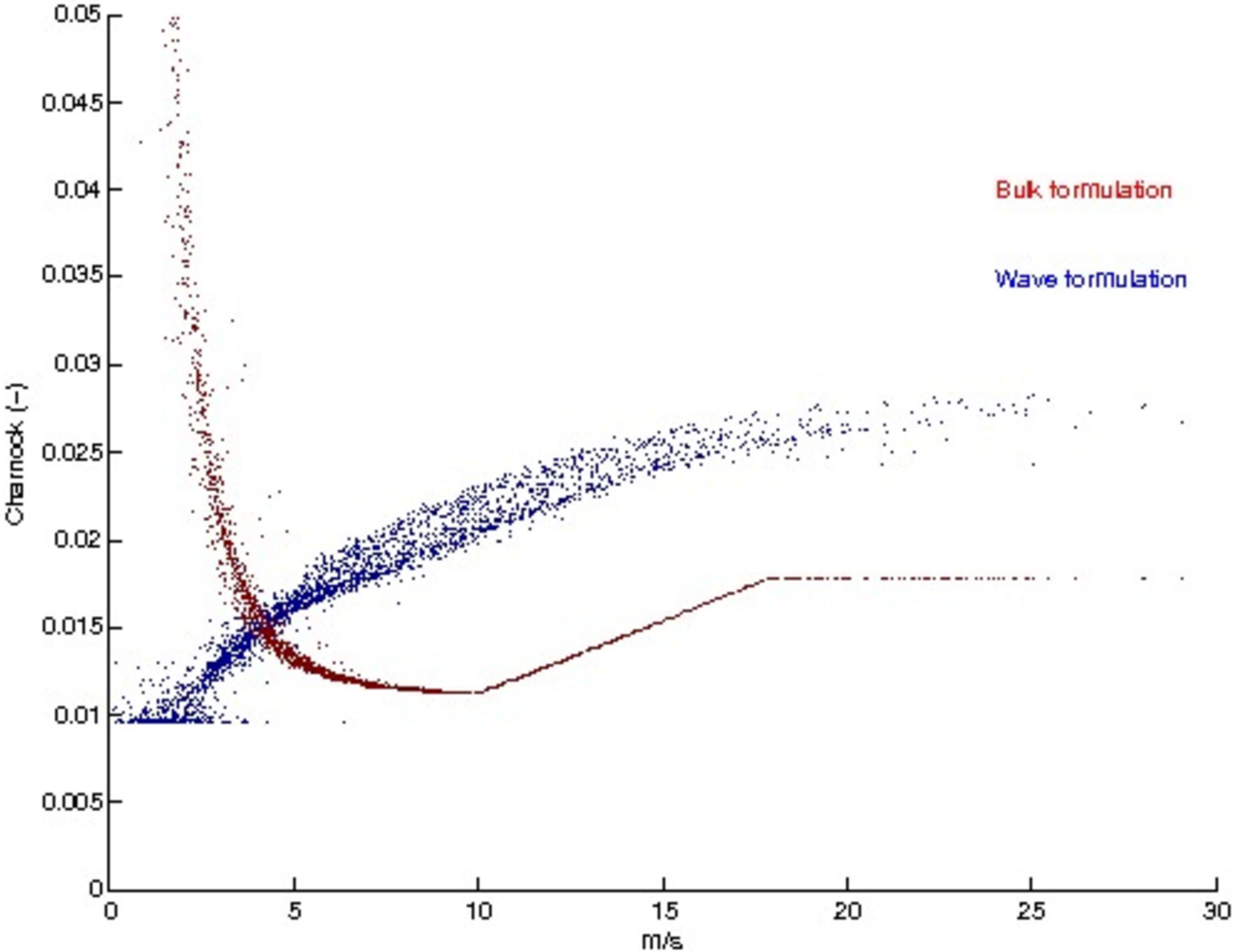

Bulk formulation
Wave formulation
Charnock (-)
m/s
0.05
0.045
0.04
0.035
0.03
0.025
0.02
0.015
0.01
0.005
0
5
10
15
20
25
30

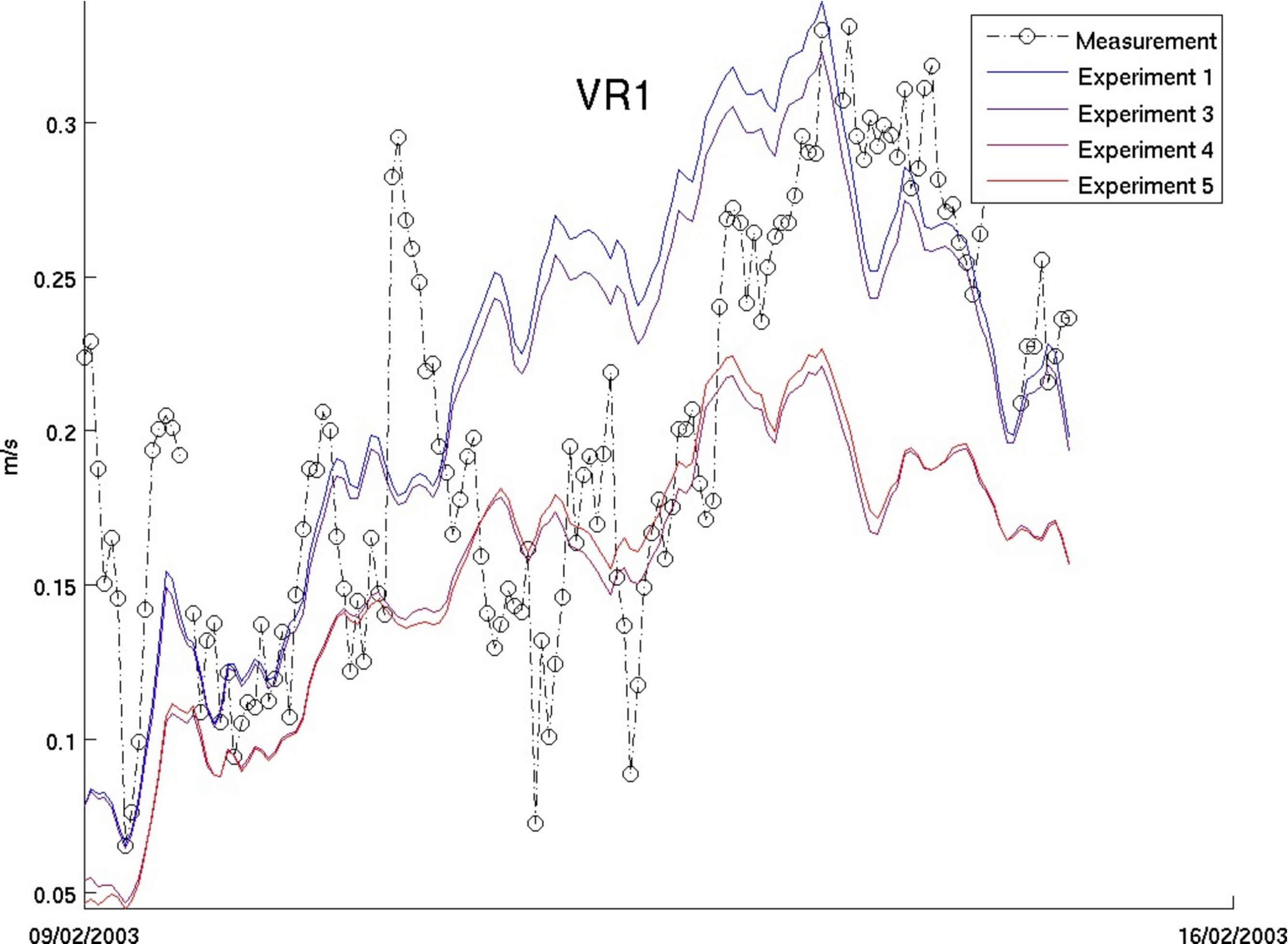
VR1
Measurement
Experiment 1
Experiment 3
Experiment 4
Experiment 5
m/s
0.3
0.25
0.2
0.15
0.1
0.05
09/02/2003
16/02/2003

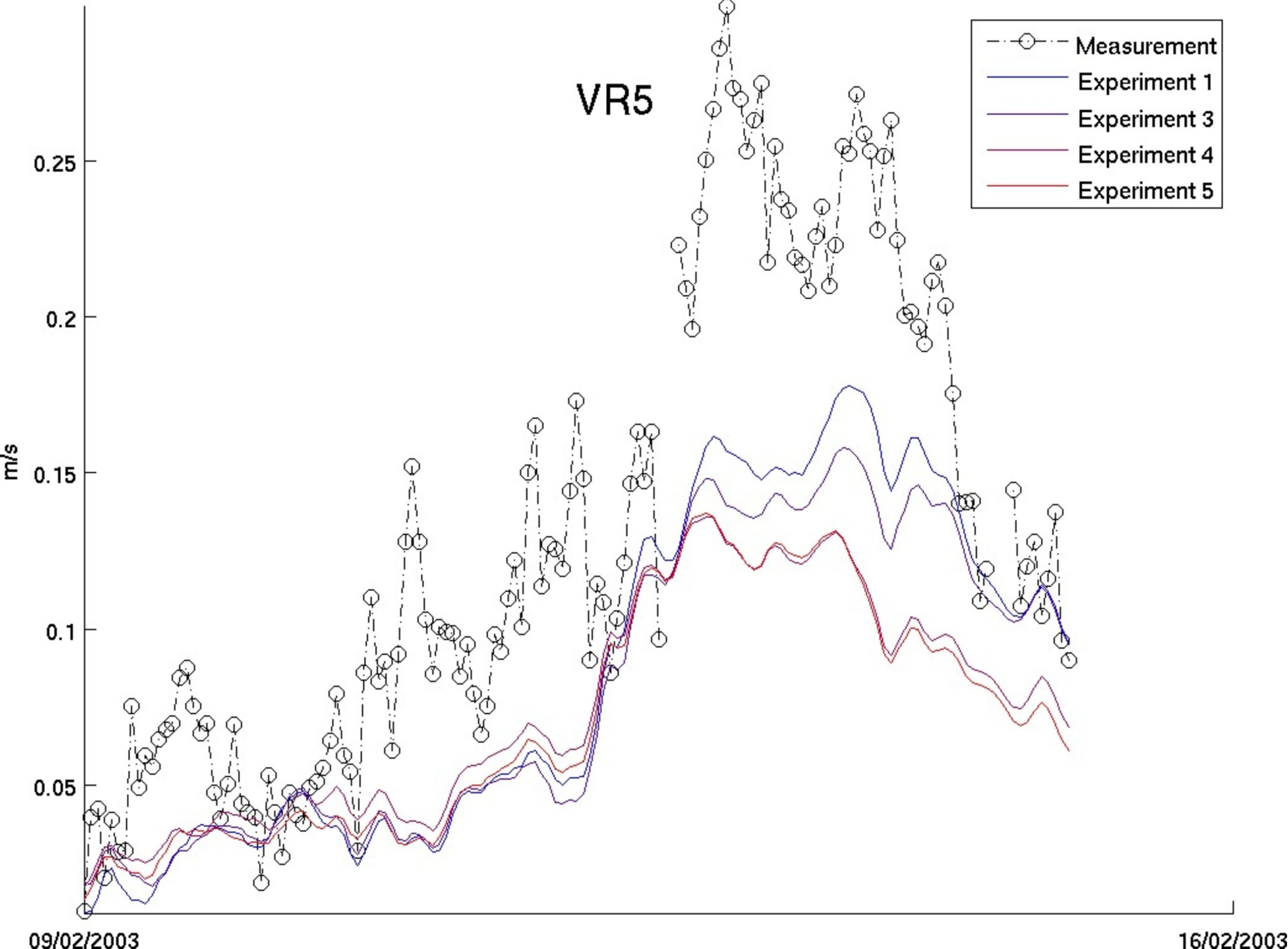
VR5
Measurement
Experiment 1
Experiment 3
Experiment 4
Experiment 5
m/s
0.25
0.2
0.15
0.1
0.05
09/02/2003
16/02/2003

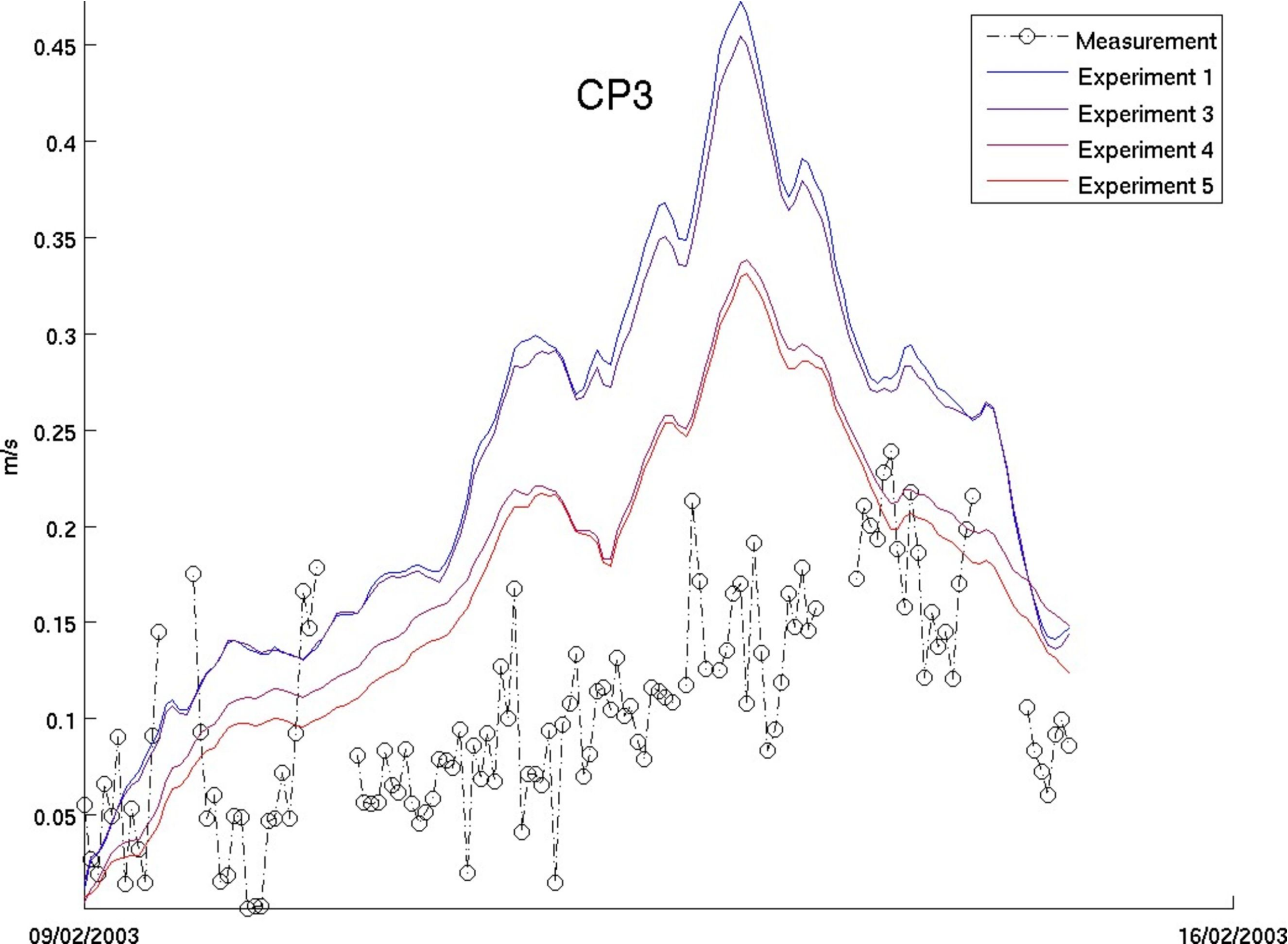
CP3
Measurement
Experiment 1
Experiment 3
Experiment 4
Experiment 5
m/s
0.45
0.4
0.35
0.3
0.25
0.2
0.15
0.1
0.05
09/02/2003
16/02/2003

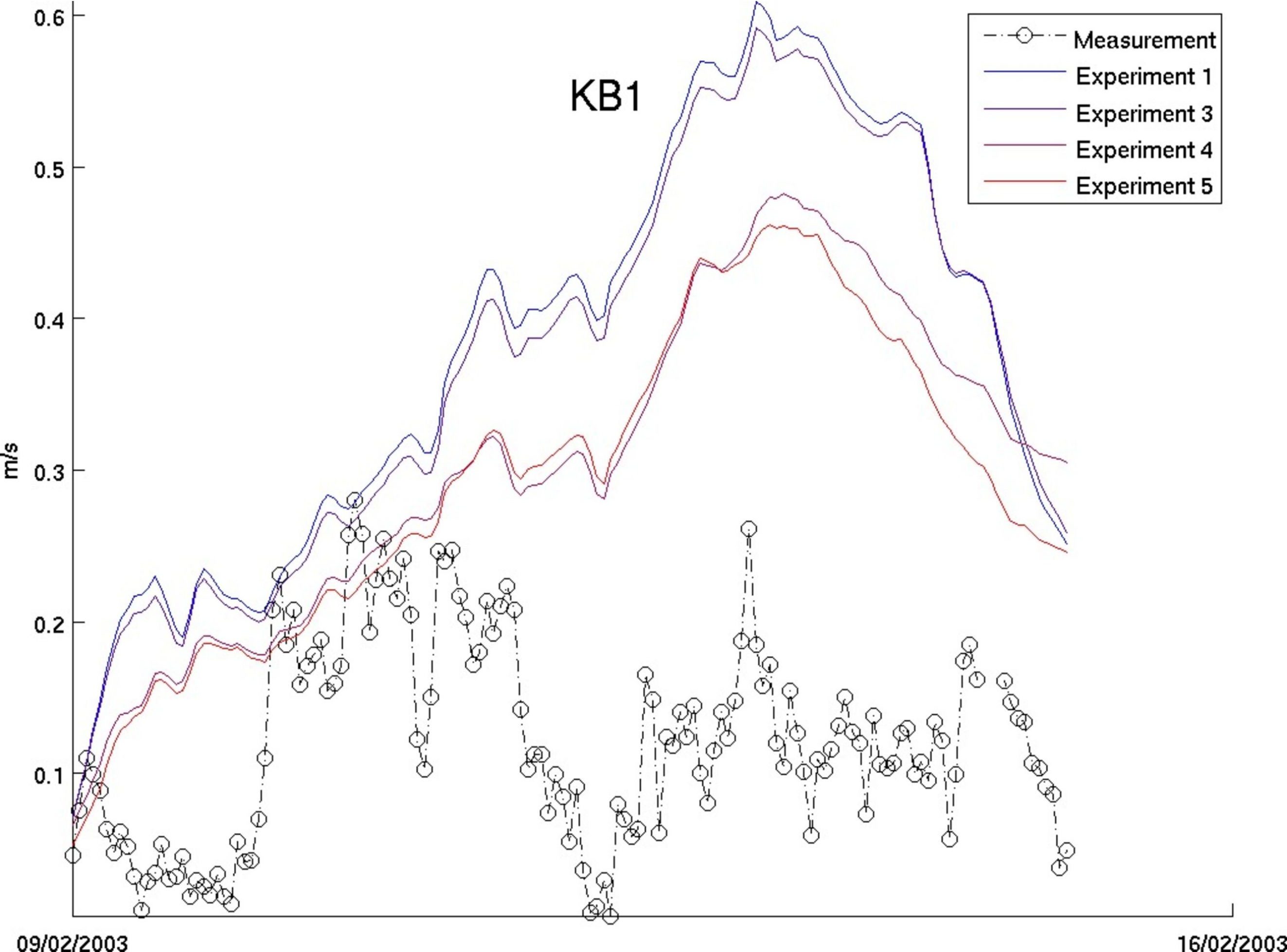

KB1
Measurement
Experiment 1
Experiment 3
Experiment 4
Experiment 5
m/s
0.6
0.5
0.4
0.3
0.2
0.1
09/02/2003
16/02/2003

Surface Stokes drift magnitude at 2003-01-01 16:00:00

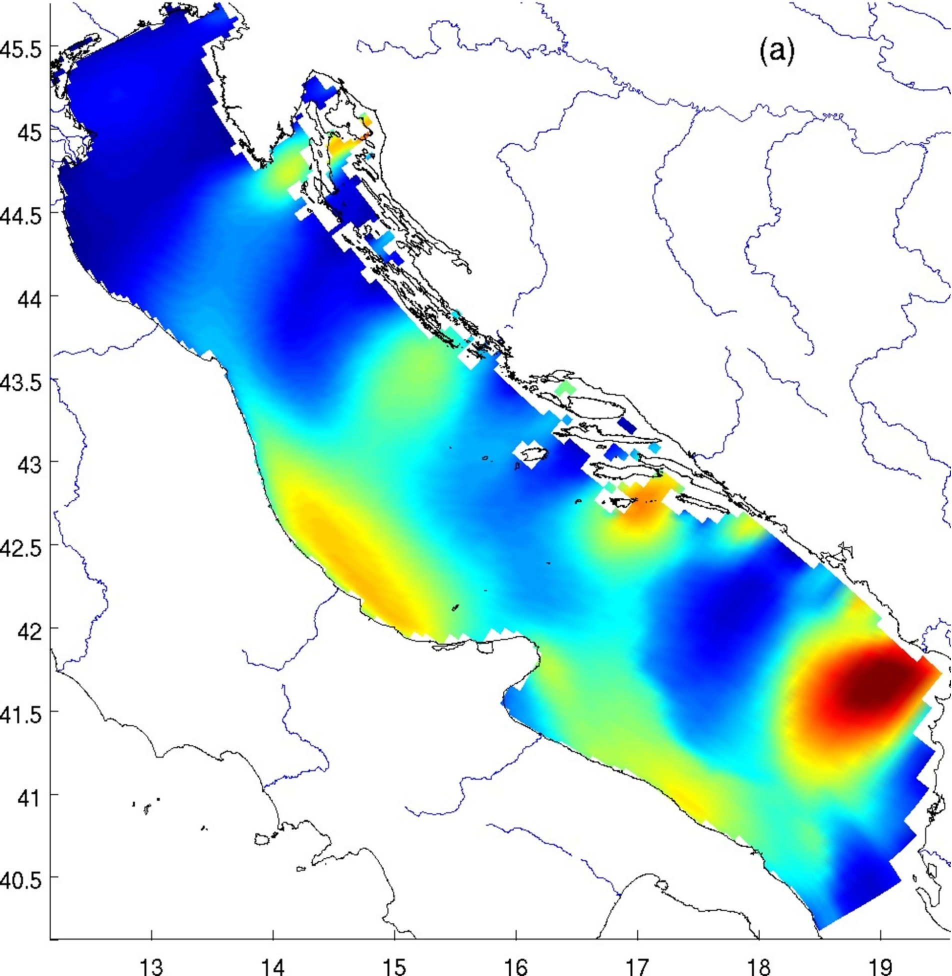

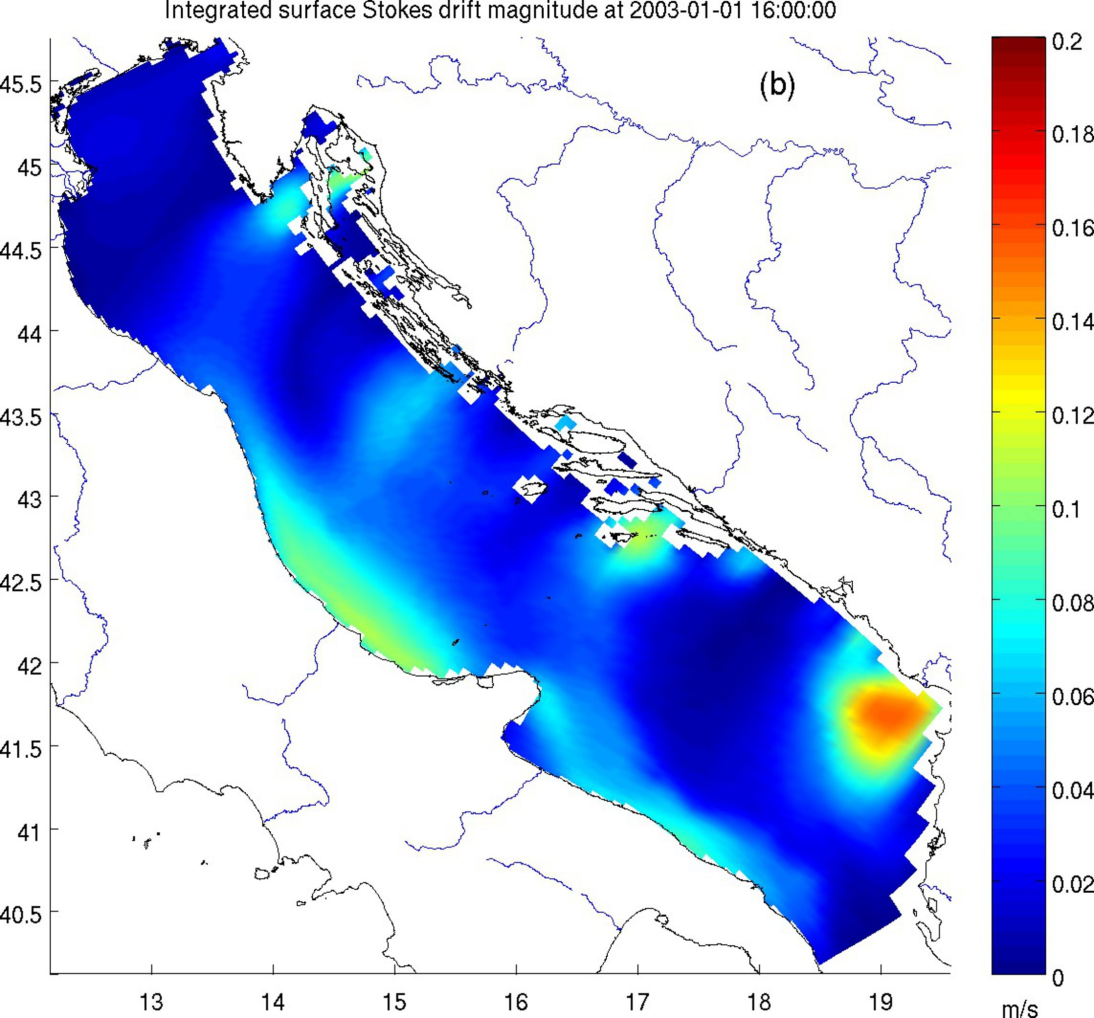
Integrated surface Stokes drift magnitude at 2003-01-01 16:00:00
(b)
45.5
45
44.5
44
43.5
43
42.5
42
41.5
41
40.5
13
14
15
16
17
18
19
0.2
0.18
0.16
0.14
0.12
0.1
0.08
0.06
0.04
0.02
0
m/s

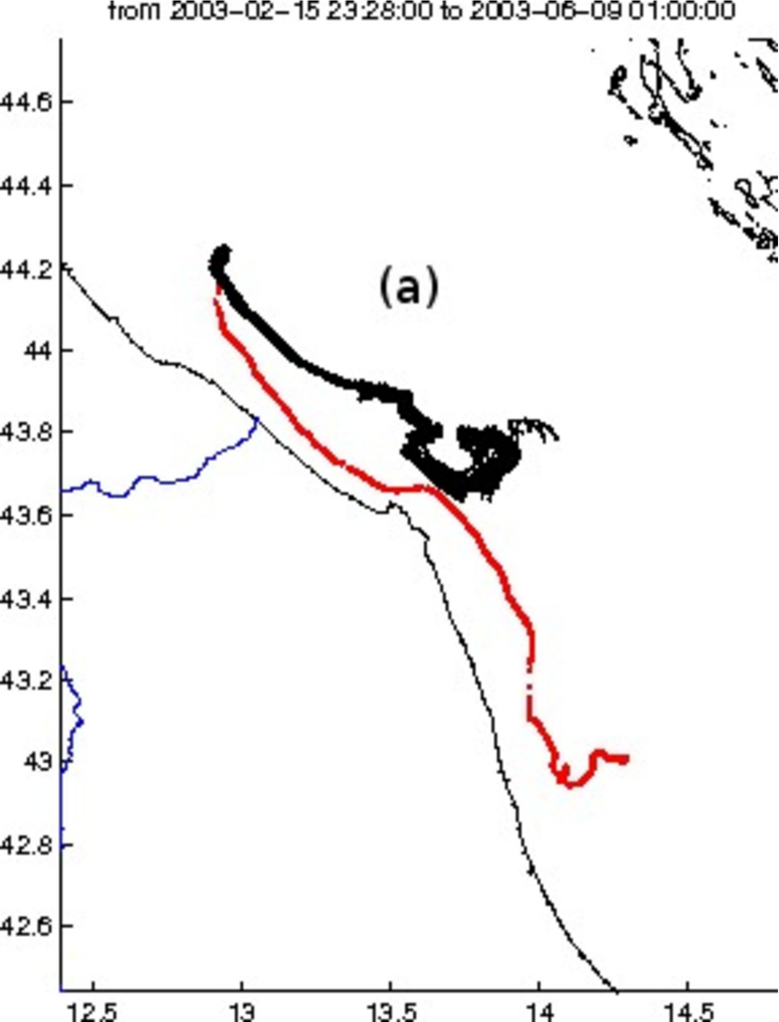

from 2003-02-15 23:28:00 to 2003-06-09 01:00:00
(a)
44.6
44.4
44.2
44
43.8
43.6
43.4
43.2
43
42.8
42.6
12.5
13
13.5
14
14.5

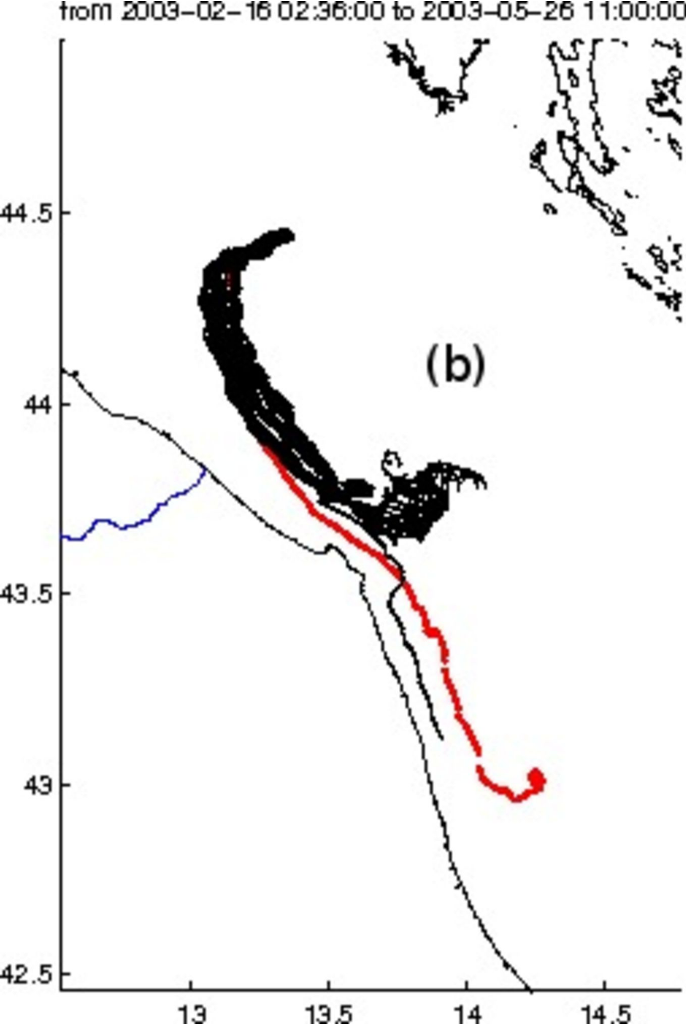

from 2003-02-16 02:36:00 to 2003-05-26 11:00:00
44.5
44
43.5
43
42.5
13
13.5
14
14.5
(b)

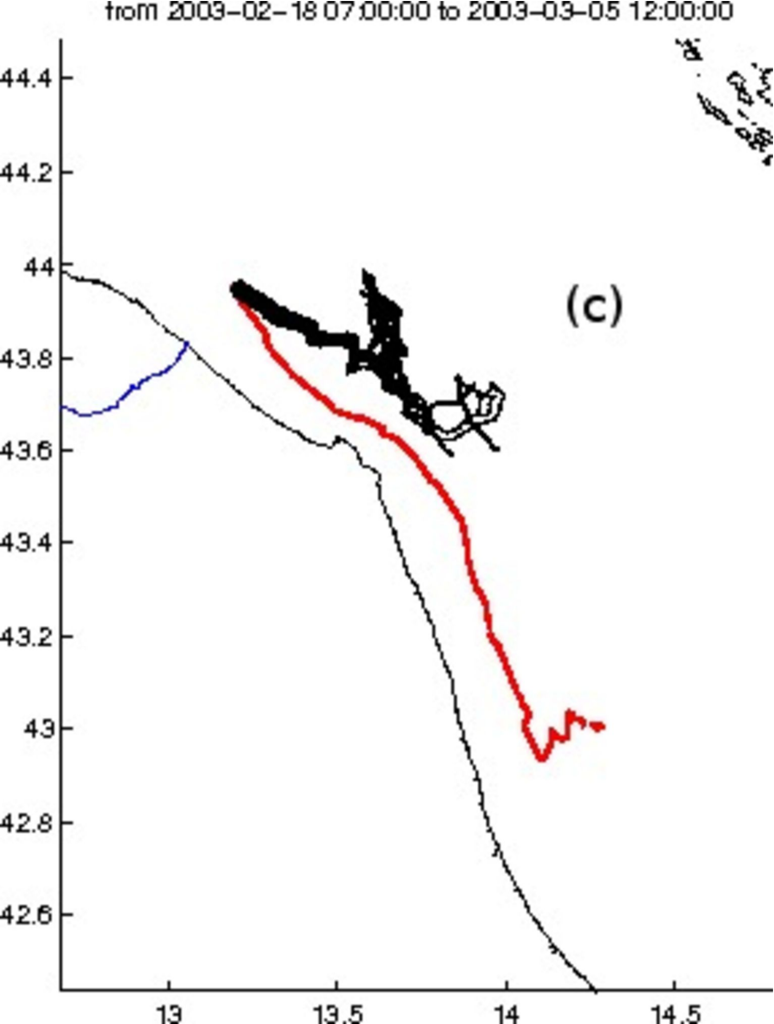
from 2003-02-18 07:00:00 to 2003-03-05 12:00:00
(c)
44.4
44.2
44
43.8
43.6
43.4
43.2
43
42.8
42.6
13
13.5
14
14.5

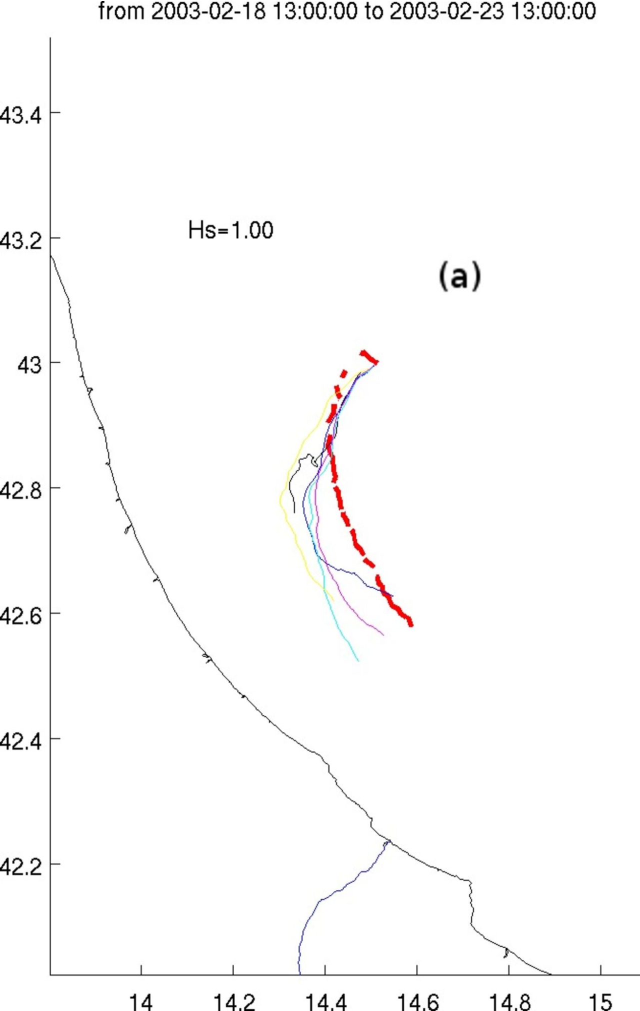
from 2003-02-18 13:00:00 to 2003-02-23 13:00:00
Hs=1.00
(a)
43.4
43.2
43
42.8
42.6
42.4
42.2
14
14.2
14.4
14.6
14.8
15

from 2003-02-13 04:00:00 to 2003-02-18 04:00:00

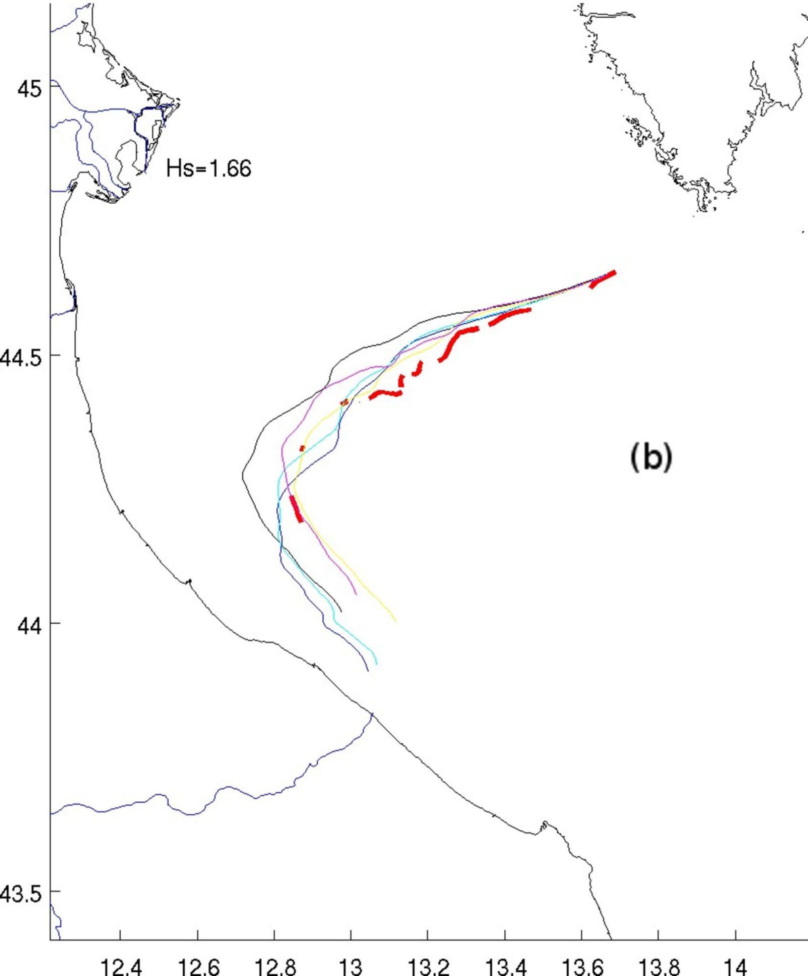

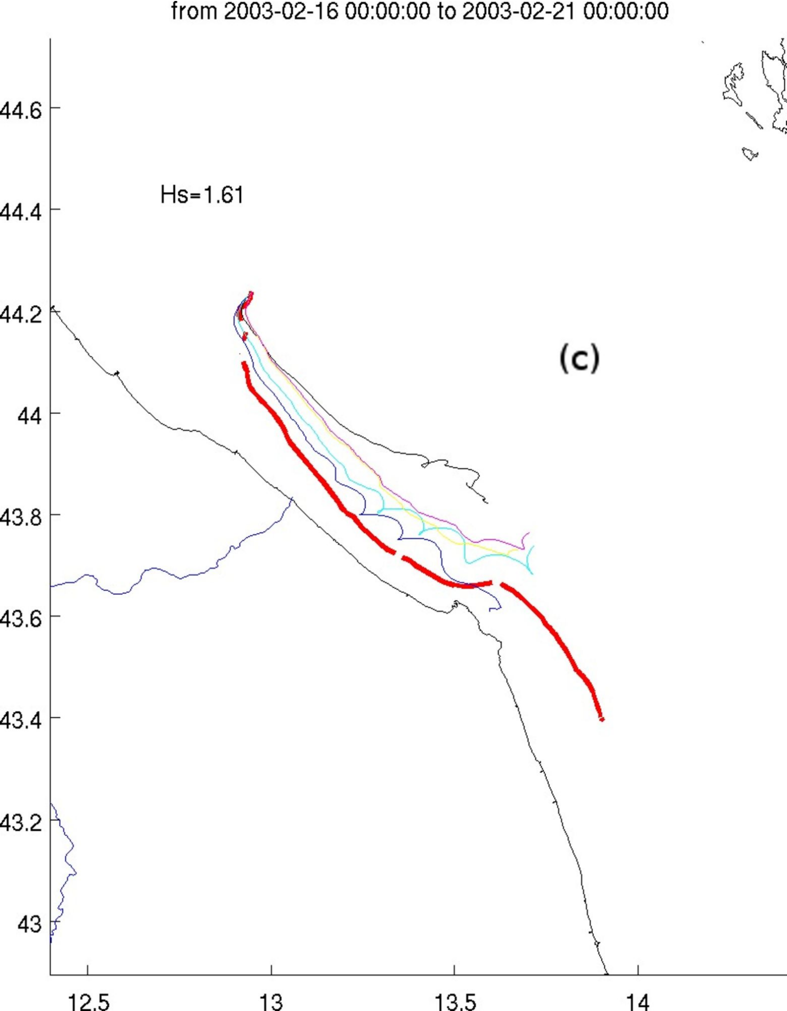
from 2003-02-16 00:00:00 to 2003-02-21 00:00:00
Hs=1.61
(c)
44.6
44.4
44.2
44
43.8
43.6
43.4
43.2
43
12.5
13
13.5
14

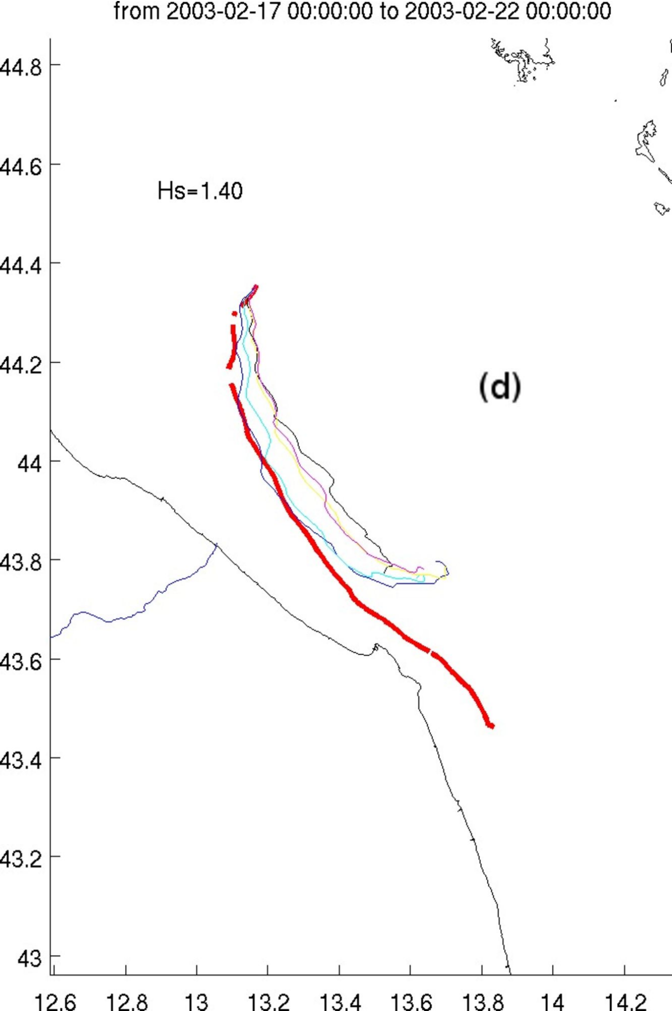

from 2003-02-17 00:00:00 to 2003-02-22 00:00:00
Hs=1.40
(d)
44.8
44.6
44.4
44.2
44
43.8
43.6
43.4
43.2
43
12.6
12.8
13
13.2
13.4
13.6
13.8
14
14.2